Conception of novel blue crab chitosan films crosslinked with different saccharides via the Maillard reaction with improved functional and biological properties

Marwa Hamdi, Rim Nasri, Youssra Ben Azaza, S.M. Li, Moncef Nasri

Conception of novel blue crab chitosan films crosslinked with different saccharides via the Maillard reaction with improved functional and biological properties

Rim Nasri, Youssra Azaza, Suming Li, Moncef Nasri, Marwa Hamdi

Conception of novel blue crab chitosan films crosslinked with different saccharides via the Maillard reaction with improved functional and biological properties.

Marwa Hamdi [a*], Rim Nasri [a,b], Youssra Ben Azaza [a], Suming Li [c], Moncef Nasri [a]

[a] Laboratory of Enzyme Engineering and Microbiology, University of Sfax, National Engineering School of Sfax, B.P. 1173, 3038 Sfax, Tunisia.

[b] Higher Institute of Biotechnology of Monastir, University of Monastir, Monastir, Tunisia.

[c] European Institute of Films, UMR CNRS 5635, University of Montpellier, Place Eugene Bataillon, 34095 Montpellier Cedex 5, France.

*** Corresponding author:** Marwa Hamdi, Laboratory of Enzyme Engineering and Microbiology, University of Sfax, National Engineering School of Sfax, B.P. 1173, 3038 Sfax, Tunisia. **Tel:** 216 25740373 / 216 54186612; **E-mail:** marwahamdi50@yahoo.fr.

Abstract

This work aimed to modify blue crab chitosan-based films through the Maillard reaction (MR) as a novel alternative to improve their functional and biological properties. To this end, different saccharides (glucose (aldohexose), fructose (ketohexose), xylose (aldopentose) and arabinose (aldopentose)), at different weight ratios 0.5, 1.0 and 2.0% (g/100 g polymer), were studied, and films were heated at 90 °C for 24 h. Based on color changes and browning index measurements, the extent of MR was the highest with aldopentoses, whereas hexoses and particularly ketohexoses, exhibited a relative crosslinking rate. These findings were further reflected with an improvement in treated films mechanical properties and thermal degradation temperatures, and advantageously, barrier properties against UV light and water. In addition, the MR-modified Cs-based films antioxidant activity was interestingly enhanced with mainly aldopentoses. Consequently, MR crosslinked chitosan-based films are promising alternative for active and functional packaging able of food oxidation hindering, especially using aldopentoses.

Keywords: Chitosan; Films; Crosslinking; Maillard reaction; *In vitro* characterization.

1. Introduction

Nowadays, there has been several concerns towards the alarming natural resources lessening, health and environmental hitches of petroleum-based synthetic polymers, traditionally and massively used in medical and food industries (Al Jahwari and Pervez, 2019; Liu *et al*., 2019; Sponchioni, Palmiero and Moscatelli, 2019). Therefore, intensive researches, in the field of food protection, has focused on the conception of a natural and non-toxic coating material, able of effectively enhancing the shelf-life of fresh or packaged commercialized food, as alternative to synthetic films (Assadpour and Jafari, 2019; Galiano *et al*., 2018).

These bio-based packaging should be able to perfectly hinder the UV radiation, prevent oxidative damages and encounter food-borne pathogens developpement, for the protection of food and extending their shelf life, without ideally loss of their mechanical integrity and behavior characteristics (Vilela *et al*., 2017). Among most studied biopolymers, chitosan is an inspiring and propitious polymer, of a polysaccharide nature, competently applied as an alternative in agriculture, food and pharmaceutical industries (Vukajlovic, Parker, Bretcanu and Novakovic, 2019; Shariatinia, 2018). Although the applicability of chitosan-based biomaterials is knowing a noteworthy increase (Zhai, Bai, Zhu, Wang and Luo, 2018), still certain physicochemical properties of the chitosan-based films are deficient and require, thereby, to be amended in order to feat industrial needs, such as light and water barrier properties, since packaging materials' water content and light (UV specially) transmission basically affected packaged or coated materials' shelf life), as well mechanical resistance (Akyuz *et al*., 2017). In fact, regarding materials applied or expected for food packaging, mechanical properties evaluation is mandatory for shaping their performance to sustain several sorts of stresses occurring during packaging applications processes.

Several types of treatments can be used for the modification of edible films, in order to improve their structural properties (such as sensitivity to water), barrier characteristics (light

barrier and water vapor or gas permeability), biological properties (i.e. antioxidant and antimicrobial activities), etc., including the combination of two polymers, physical treatments such as heat treatment and irradiation and biochemical treatments such as the Maillard reaction (MR) (Mujtaba *et al*., 2019; Kamboj, Singh, Tiwary and Rana, 2015).

Given the good antioxidant and antibacterial activities of MR products in food industry, their use as a preservative is attracting increasing interest (Sung, Chang, Chou and Hsiao, 2018; Cai *et al*., 2016; Gullon *et al*., 2016; Wu *et al*., 2014). The MR, also called non-enzymatic browning, is a chemical reaction of browning of amino acids in the presence of sugars (Umemura and Kawai, 2007). MR is the main reaction responsible for the transformation of precursors into dyes and flavoring compounds during food processing and preservation (Xu, Huang, Xu, Liu and Xiao, 2019), which can be influenced by many factors, including reagent concentration, temperature, heating time, initial pH, and reagent characteristics.

In a previous work (Hamdi, Nasri, Li and Nasri, 2019a), the improvement of the barrier, mechanical and biological properties of blue crab chitosan-based films was envisaged, by incorporation of carotenoproteins used both as polymers and antioxidant and antimicrobial agents. The addition of carotenoproteins at 15% (w/w Cs) in the blue crab chitosan film-forming matrix allowed an improvement in the barrier, color, thermal and biological (antioxidant and antimicrobial) properties. However, a reduction in their mechanical resistance was noted. Thus, the present work is interested in a novel alternative to improve the physical and biological properties of blue crab chitosan-based films, by complex crosslinking coupled with a heat treatment. Indeed, recently, researches regarding modifying proteins properties through the MR revealed that protein-saccharide grafts are advantageous as an innovative functional biopolymer with excellent emulsifying, antioxidant and antimicrobial properties for food and pharmaceutical applications (Kchaou *et al*., 2018).

Although many studies, dealing with chitosan-based films (Fernandez-de Castro *et al*., 2016; Rubentheren *et al*., 2016; Leceta, Guerrero, Ibarburu, Dueñas and de la Caba, 2013) and chitosan-MR (Wang, Liu, Liang, Yuan and Gao, 2014; Lakshmi Kosaraju, Weerakkody and Augustin, 2010; Umemura and Kawai, 2008), have been performed, and the factors affecting the reaction, including sugar concentration, temperature and reaction time have been evaluated (Gullon *et al*., 2016), there are no many previous reports on the effect of saccharides type/chemical structure on the physicochemical and antioxidant properties of films based on chitosans and different types of saccharides. Therefore, in the present work, we have chosen to compare the reactivity of chitosan with different mono-saccharides, glucose (aldohexose), fructose (ketohexose), xylose (aldopentose) and arabinose (aldopentose), at different weight ratios 0.5, 1.0 and 2.0% (g/100 g polymer).

2. Materials and methods

2.1. Materials

D-anhydrous-glucose ($C_6H_{12}O_6$; 180 g mol^{-1}), D-anhydrous fructose ($C_6H_{12}O_6$; 180 g mol^{-1}), L-anhydrous-arabinose ($C_5H_{10}O_5$; 150 g mol^{-1}) and L-anhydrous-xylose ($C_5H_{10}O_5$; 150 g mol^{-1}), purchased from Sigma-Aldrich (France), were applied as reducing sugar for the Maillard reaction initiation in Cs-based films. In the present work, the other used chemical reagents from commercial sources were of analytical grade and employed without further purifications.

2.2. Extraction of blue crab chitosan

Chitosan (Cs), with acetylation degree of 8%, as characterized by ^{13}C NMR, molecular weight Mw of 115 kDa and intrinsic viscosity [η] of 3432 ml/g, based on the size exclusion chromatography, was obtained from blue crab shells chitin, through N-deacetylation with NaOH

12.5 M, at a ratio of 1/10 (w/v), for 4 h at 140 °C, as reported in our previous study (Hamdi *et al*., 2018).

2.3. Preparation of Cs-based MR-treated films

Film-forming solutions were prepared by dissolving Cs at a concentration of 2% (w/v) in aqueous solution of acetic acid 0.15 M. Then, sugars (glucose, fructose, arabinose and xylose) were added under gentle stirring at different concentrations (0.5, 1.0 and 2.0%; w/w dry Cs matter). Glycerol was added as a plasticizer to the film-forming solutions at a concentration of 15% (w/w dry Cs matter). After stirring for 24 h at 25 °C and degassing, film-forming solutions were left standing for 12 h at 25 °C and centrifuged for 10 min at 8000 g. Thereafter, films were prepared by casting film-forming solutions (25 ml) on Petri dishes (13.5 cm diameter) and were left to dry for 48 h at 25 °C, until complete solvent evaporation.

The well-dried films were peeled from the plate and heated for 24 h in an oven at a temperature of 90 ± 2 °C and an average relative humidity (RH) value of approximatively 30%, to apply the heat-treatment for MR induction. Non-heated films are considered as controls and saccharide-free chitosan film is considered as blank. Finally, all designed films were maintained at 25 °C at a RH of 50%, for subsequent characterizations.

2.4. Analytical methods

2.4.1. Films thickness

The thickness of prepared films was measured by using a micrometer (Digimatic IP65, Mitutoyo, France), reporting the average value of 5-6 measurements taken at random locations. Thickness results were taken into account for mechanical properties.

2.4.2. Films moisture content

Water content (WC) of prepared films was performed in an oven at 105 °C, where samples (approximately 100 mg) were dried until constant weight was reached (sample dry

136 weight). The moisture content of films was determined by measuring the mass loss of each film
137 in triplicate and expressed as follows [21]:

138 $$\mathrm{WC}\ (\%) = \frac{\mathrm{M_0} - \mathrm{M_1}}{\mathrm{M_0}} \times 100 \qquad \boldsymbol{Eq}\ (\mathbf{1})$$

139 where M_0 and M_1 are respective weights (g) of films before and after drying.

140 **2.4.3. Films water solubility**

141 Films solubility in water was determined in triplicate based on the method reported by
142 Gennadios, Handa, Froning, Weller and Hanna (1998). Film samples (2 cm x 5 cm; about 100
143 mg), previously weighed, were immersed in 30 ml distilled water containing 0.1% (w/v)
144 antimicrobial agent (sodium azide), for 24 h at 25 °C. Afterwards, tubes containing film samples
145 were centrifuged at 3000 g, 25 °C for 10 min. Supernatants were removed, and solubilized film
146 portion was estimated by drying the obtained undissolved debris, at 105 ° C for 24 h. Water
147 solubility (WS) was determined according the following equation:

148 $$\mathrm{WS}\ (\%) = \frac{[\mathrm{M_i} \times (100 - \mathrm{WC}) - \mathrm{M_f}]}{\mathrm{M_i} \times (100 - \mathrm{WC})} \times 100 \qquad \boldsymbol{Eq}\ (\mathbf{2})$$

149 where M_i and M_f are initial and final respective masses (g) of films and WC is water content of
150 each film sample (%).

151 **2.4.4. Films water contact angle**

152 A goniometer (Drop Shape Analyzer 30 from Kruss GmbH), equipped with an image
153 analysis software (ADVANCE) was used for the study of the films water contact angle (WCA),
154 considering the sessile drop method. Briefly, a droplet of water (approximatively 2 ml) was
155 dropped on the film surface using a precision syringe, in an environmental chamber with a
156 constant environment at a temperature of 25 ± 2 °C and a RH of 50%. WCA, expressed as °,

was measured on both sides of the drop and the average of five measurements was determined and reported.

2.4.5. Films water vapor permeability

The gravimetric method, adapted by Debeaufort, Martin-Polo and Voilley (1993) for hydrophilic polymers, was applied for the determination of films water vapor permeability (WVP). First, to permit films equilibration, samples were conditioned at 25 °C and 50% RH for a minimum equilibration time of 48 h. Films thickness measurements values and statistical error were considered in the WVP measurements. WVP calculations were based on maintaining film samples between two Teflon rings at the glass cell upper. The WVP cell containing KCl saline solution (100% RH), was placed into a climatic chamber (KBF 240 Binder, ODIL, France) maintained at 25 °C and a RH of 30%. Once the equilibrium state was reached, the value of WVP (g m^{-1} s^{-1} Pa^{-1}) was calculated, based on the change in the absolute value of the weight loss as a function of time, as follows:

$$\text{WVP}\ (\text{g m}^{-1}\ \text{s}^{-1}\ \text{Pa}^{-1}) = \frac{\Delta \text{m}}{\Delta \text{t}} \times \frac{1}{\text{A}} \times \frac{1}{\Delta \text{p}} \times \text{e} \qquad \boldsymbol{Eq\ (3)}$$

where $\Delta m/\Delta t$ is the weight of moisture loss per unit of time (g/s), A is the film area exposed to the transfer (1.39×10^4 m^2), e is the film thickness (m), and Δp is the water vapor partial pressure differential between the two sides of the film (Pa).

2.4.6. Optical properties of films

2.4.6.1. Color features

Films color parameters were measured, using a portable colorimeter (Minolta Chroma Meter CR-300, CIE, 1976) and the color was recorded using the color parameters CIE L* a* b*. L* indicates transparency and its value varies from 0 (black) to 100 (white), a* is a measure of green (-a*) / redness (+ a*) and b* is the measure of blue (-b*) / yellow (+ b*). The

colorimeter was calibrated against a standard Minolta standard reflector plate before each actual color measurement. In addition, for the derived color parameters, the total color difference (ΔE), of prepared films were calculated using the following equations:

$$\Delta E = \sqrt{(L^* - L_0{}^*)^2 + (a^* - a_0{}^*)^2 + (b^* - b_0{}^*)^2} \qquad \textbf{Eq (4)}$$

where L_0*, a_0*, b_0* are the colorimetric parameters of the standard are (L* = 97.25, a* = -0.2 and b* = 2.25) and L*, a*, b* are the values for the films obtained. The C axis represents Chroma (or saturation). It ranges from 0, which is completely unsaturated (neutral gray, black or white) to 100 for very high Chroma (saturation) or purity of color.

2.4.6.2. Maillard-treated films browning index

Films browning index (BI) was determined, as reported by Matiacevich and Pilar Buera (2006), based on the CIE L* a* b* values, using the following equation:

$$BI = \frac{100\ (z - 0.31)}{0.172} \qquad \textbf{Eq (5)}$$

where,

$$z = {a + 1.75\ (L)}\Big/{5.645\ (L) + a - 3.012\ (b)} \qquad \textbf{Eq (6)}$$

2.4.6.3. Films UV barrier and transparency properties

The transmittance spectra (200-800 nm) of the developed films were made using a UV-Visible spectrophotometer (T70, UV/vis spectrometer, PG Instruments Ltd., China). Thus, the films are cut to obtain rectangles of 1 cm x 3 cm and directly placed in the test cell of the spectrophotometer. Air was used as a reference. This measurement aims to evaluate the barrier effect of UV films and to determine their transparency, considering the following equation:

$$\text{Transparency}\ (\%) = \frac{-\log T_{600}}{e} \qquad \textbf{Eq (7)}$$

where T_{600} is the fractional transmittance at 600 nm and e is the thickness (mm) of the films. The lower transparency of the film is reflected by a greater transparency value.

2.4.7. Infrared spectroscopy analysis

The FT-IR spectra of the prepared were performed using a spectrometer (Agilent Technologies, Carry 630 series) equipped with an attenuated reflection accessory (ATR) containing a diamond/ZnSe crystal, at room temperature (25 °C) in the spectral range frequencies of 650-4000 cm^{-1}. For each spectrum, 32 scans of interferograms were averaged and the spectral resolution was 4 cm^{-1}. Data analysis and treatment was carried out by using the OMNIC Spectra software (ThermoFisher Scientific).

2.4.8. Films thermal properties

2.4.8.1. Differential Scanning Calorimeter analysis

Differential Scanning Calorimeter (Modulated DSC Q20, TA Instruments), equipped with a liquid nitrogen cooling system, was used to investigate the thermal properties of prepared films, allowing the estimation of melting and crystallization point, as well as the glass transition of the macromolecular materials. Film samples were accurately weighed into aluminum pans and sealed. An empty capsule served as an inert reference and the apparatus was calibrated using indium. The thermal profile of chitosan samples was analyzed in a temperature range of 0-225 °C, at a heating rate scan of 10 °C/min, under nitrogen flow rate of 50 ml/min. Thermograms were then analyzed by using TA Universal V4.5A software.

2.4.8.2. Thermogravimetric analysis

Thermogravimetric analysis (TGA Q500 High Resolution, TA Instruments), operating under nitrogen flow, was used to study the thermal stability of Cs-based MR-treated films. The progressive change in mass (%) as a function of temperature, is recorded. Thus, films (approximatively 4 mg) were heated from 25 to 700 °C at a heating rate of 20 °C/min and

constantly measured with an accuracy of 0.01 mg. Cs-based films thermograms were subsequently recorded, analyzed and treated using the TA Universal V4.5A software (TA Instruments, Waters, New Castle, UK).

2.4.9. Films mechanical properties

Films mechanical properties were investigated based on the determination of the tensile strength (TS, MPa) and elongation at break (EAB, %) parameters. A rheometer apparatus (Physica MCR, Anton Paar, GmbH, France) equipped with mechanical properties measuring geometry was used. To this end, films rectangular samples (1.0 cm x 4.5 cm) were cut with an accurate width and parallel sides throughout the entire length.

Prior to analysis, all the films samples were equilibrated at 25 °C and 50% RH for two weeks and their thickness were measured. Based on the ISO standard, equilibrated films samples, retained in the extension grips of the measuring system, were subjected to a uniaxial tensile test, with a deformation rate of 5 mm/min until breaking. Rheoplus software was used for the estimation of TS and EAB, corresponding respectively to the maximum load and the final extension at break from the stress-strain curves. Average values from at least six measurements were reported.

2.4.10. Films microstructure

The cross-section of films was determined using scanning electron microscopy (SEM) (Hitachi S4800), at an angle of 90 ° to the surface. Prior to imaging the film cross-section, film samples were cryofractured by immersion in liquid nitrogen, cut and fixed on the SEM support using double side adhesive tape, under an accelerating voltage of 2.0 kV and an absolute pressure of 60 Pa, after sputter coating with a 5 nm thick gold.

2.5. Films antioxidant potential

2.5.1. 1,1-diphenyl-2-picrylhydrazyl (DPPH) radicals scavenging ability

The ability of films (10 mg) to scavenge DPPH radical was determined according to the method of Bersuder, Hole and Smith (1998). The absorbance change, at 517 nm between the control and the sample, was used to calculate the scavenging activity. DPPH radical-scavenging activity of Cs-based MR-treated films was evaluated and computed considering the following equation:

$$\text{DPPH Radical scavenging activity (\%)} = \frac{A_C + A_B - A_R}{A_C} \times 100 \qquad \boldsymbol{Eq\ (8)}$$

where A_C is the absorbance of the control reaction, A_R and A_B were the absorbances of Cs-based films in the reaction mixture and without addition of DPPH solution, respectively. Results were expressed as means of experiments performed in duplicate.

2.5.2. Reducing power activity assay

The ability of films (10 mg) to reduce iron (III) was determined according to the method of Yildirim, Mavi and Kara (2001). The absorbance of the resulting solutions was measured at 700 nm, after incubation at room temperature for 10 min. Higher absorbance of the reaction mixture indicated higher reducing power. The test was carried out in duplicate and BHA was used as a standard.

2.5.3. Metal-chelating activity

The chelating activity of films (10 mg) towards ferrous ion (Fe^{2+}) was studied as reported by Decker and Welch (1990). EDTA was used as reference and the chelating activity (%) was computed using the following equation:

$$\text{Chelating activity (\%)} = \frac{A_C + A_B - A_R}{A_C} \times 100 \qquad \boldsymbol{Eq\ (9)}$$

where A_C is the absorbance of the control reaction, A_R and A_B were the absorbance of Cs-based films in the reaction mixture and without addition of Ferrozine solution, respectively. Results were expressed as means of experiments performed in duplicate.

2.6. Statistical analysis

All experiments were carried out in duplicate, excepting films mechanical properties, where analysis was repeated at least six times, and average values with standard deviation errors were reported. Mean separation and significance were analyzed using the SPSS software package ver. 17.0 professional edition (SPSS, Inc., Chicago, IL, USA) using ANOVA analysis. Differences between the different Cs-based films crosslinked with the different saccharides and heated or not at 90 °C for 24 h, were considered significant at $p < 0.05$.

3. Results and Discussion

3.1. Water resistance and barrier features of Cs-based films as influenced by the MR

3.1.1. Water content measurement

Packaged or coated materials' shelf life is affected by packaging materials' WC (Kchaou *et al*., 2018). WC values (**Fig. 1A**) reveal that, for non-heated Cs-based films, humidity values increased from 20% for blank (non-added) Cs-based film to 24% for 2.0% (w/w Cs) crosslinked Cs-saccharides films ($p<0.05$), independently of the added saccharide (aldose or ketose, pentose or hexose). However, at concentrations of 0.5 and 1.0% (w/w Cs), no significant differences were noted ($p>0.05$). The very well-known hygroscopicity of saccharides could explain the increase of WC of the non-heated Cs-saccharides films (Hazaveh, Mohammadi Nafchi and Abbaspour, 2015).

After induction of the MR (heat treatment at 90 °C for 24 h), WC decreased gradually with the increase of saccharide content from 0.5% (w/w Cs) to 2.0% (w/w Cs), depending on the type of the saccharide used ($p<0.05$), due to the interaction between the amino groups of Cs and the carbonyl groups of the tested saccharide, resulting in polar groups decrease and the disruption of Cs-water interactions due to hampering of the hydroxyl and amino groups availability (Rui *et al*., 2017). In fact, regarding the Cs-arabinose crosslinked films, the WC dropped to 18.15%, 17.08% and 16.38% at 0.5, 1.0 and 2.0% (w/w Cs), which could be

explained by free water loss from MR-treated films after being heated at 90 °C. Moreover, the following order of reactivity could be observed: fructose < glucose < xylose < arabinose. For example, at a concentration of 2.0% (w/w Cs), after heat treatment, the WC values reached 16.38%, 16.73%, 17.92% and 18.39%, for Cs-arabinose, Cs-xylose, Cs-glucose and Cs-fructose crosslinked films, respectively, *vs.* 18.37% for blank Cs-based film.

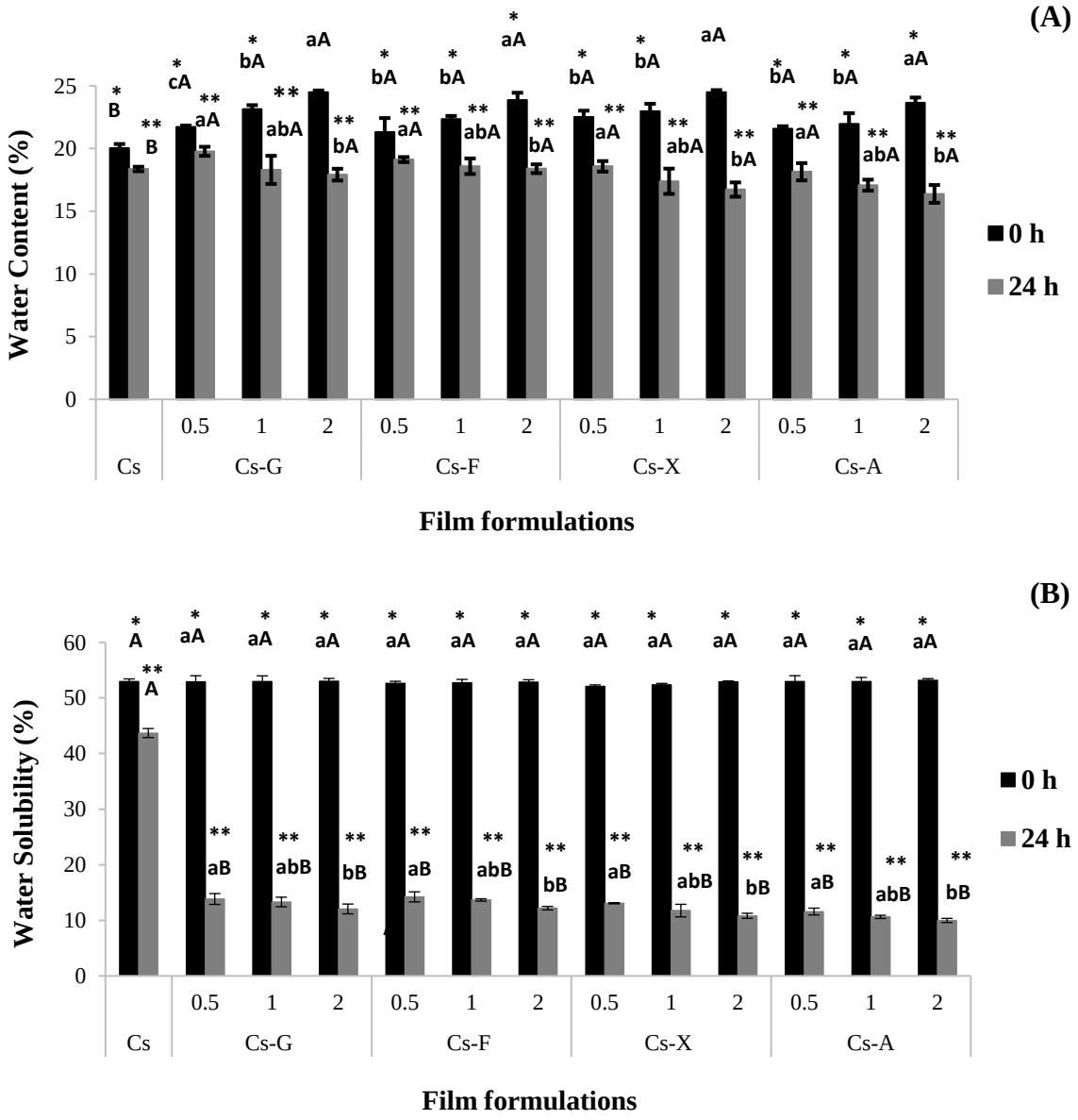

Figure 1: Water content (WC%) **(A)** and water solubility (WS%) **(B)** of Cs-based films conjugated with different saccharides, at different mass ratios (0.5, 1.0 and 2.0 %; w/w Cs), through MR at 90 °C as a function of time (0 and 24 h). **Cs:** Chitosan, **A:** Arabinose, **F:** Fructose, **G:** Glucose, **X:** Xylose. Different letters $^{(a-c)}$ in the same films group are significantly different as determined by ANOVA test ($p<0.05$). Different letters $^{(A-B)}$ indicated significant differences between different films groups at the same heating time ($p<0.05$). Different symbols $^{(*-**)}$ indicated significant differences between heated and non-heated films for the same group ($p<0.05$).

311 This finding suggested that the extent of the MR, as reflected by films water content
312 decrease, was influenced by the type of saccharides, where pentoses (arabinose and xylose),
313 with less carbons in their macromolecular chain, showed more reactivity, compared to the
314 hexoses (fructose and glucose), with more carbons (Gullon *et al*., 2016). Particularly, aldoses
315 (arabinose, xylose and glucose), with a carbonyl group located at one end of the carbon chain,
316 were more reactive than ketoses (fructose), with a carbonyl group situated inside the carbon
317 chain, resulting in the lowest WC values after crosslinking with aldopentoses, proving higher
318 covalent crosslinking extent and lower polar groups availability.

319 **3.1.2. Study of water solubility**

320 Films WS, related with the biomaterial hydrophobicity/hydrophilicity, is a crucial feature
321 defining biopolymeric-based films applications. WS results, shown in **Fig. 1B**, highlight that
322 blank Cs-based film was sensitive to water, exhibiting WS of 52%. For the non-heated Cs-
323 saccharides films, WS values were maintained constant, independently of the type and dose of
324 added saccharide, compared to the blank Cs-based film ($p>0.05$). However, as expected, due to
325 the crosslinking, films WS decreased significantly with the heat treatment for the different Cs-
326 saccharide ratios ($p<0.05$). For example, after 24 h MR time, WS reached values of 11.58%,
327 10.62% and 9.98% for Cs-arabinose mass ratios of 0.5, 1.0 and 2.0% (w/w Cs), respectively,
328 *vs.* 43.69 for blank Cs-based film heated at 90 °C for 24 h. Compared to blank film, when added
329 to the Cs film-forming solution, overall tested saccharides acted as crosslinking agent,
330 permitting the creation of covalent bonds with the Cs polymeric matrix, and thereby, the
331 decrease of WS values (Kamboj *et al*., 2015). In fact, the principal mechanisms of MR are the
332 formation of the initial products, called Schiff bases, which form Amadori products via
333 rearrangement. These latter undergo further reactions to form irreversible advanced glycation
334 end products, called melanoidins (Kchaou *et al*., 2018).

Moreover, WS decrease was saccharide dose dependent. In fact, WS of films with higher saccharide contents (2.0%, w/w Cs), and thereby, higher crosslinking rate, decreased more rapidly, compared to films with relative crosslinking degree, as a result of lower saccharide content (0.5%, w/w Cs).

As predicted, MR was more facilitated with pentoses and aldoses than hexoses and ketoses, knowing that higher crosslinking resulted in lower the solubility. For 2.0% (w/w Cs), Cs-arabinose MR-treated films displayed the lowest WS values of 9.98%, followed by Cs-xylose, Cs-glucose and Cs-fructose MR-treated films ($p<0.05$), with respective WS of 10.81%, 12.05% and 12.19% (**Fig. 1B**). Average WS values of 52% were initially recorded for non-heated films. This increase in MR-treated films insolubility in water, depending on the type and dose of added saccharide, could be the result of higher covalent crosslinking extent, particularly in the presence of aldopentoses. More precisely, this higher WS of the resulting films due to higher glycation rate (the extent of crosslinking between amino groups of Cs and the carbonyl groups of the tested saccharide) could be ascribed to the formation of melanoidins (heterogeneous brown polymers of high molecular weight), non-soluble MR compounds (Stevenson *et al.*, 2020).

Based on the latter outcomes, MR, mainly *via* crosslinking with aldopentoses, could be considered as effective alternative allowing the amelioration of Cs-based films water resistance in terms of their insolubility in water.

3.1.3. Water contact angle determination

One of the common ways to measure the wettability (resistance to water absorption) of films surface is the determination of WCA, indicating, the hydrophilicity/hydrophobicity degree of films (Etxabide, Uranga, Guerrero and de la Caba, 2015). Obtained data are reported in **Table 1** and **Supplementary Data Fig. S1**.

359 **Table 1:** Water contact angle (WCA), water vapor (WVP) permeability, tensile strength (TS)
360 and elongation at break (EAB) of Cs-based MR-treated films, compared to the non-modified
361 control film.

Film formulations		MR heating time (h)	WCA (°)	WVP 10^{-10} (g m^{-1} s^{-1} Pa^{-1})	TS (MPa)	EAB (%)
Cs		0	92.4±0.6 ^{aA}	3.6±0.1 ^{aB}	18.9±0.5 ^{aA}	29.6±0.4 ^{aA}
		24	91.5±0 ^{aH}	3.4±0.3 ^{aA}	18.7±0.9 ^{aF}	29.8±0.8 ^{aF}
Cs-G	**0.5**	0	92.8±0.2 ^{aA}	3.8±0.9 ^{aAB}	18.6±0.4 ^{aA}	29.9±0.7 ^{aA}
		24	100.8±1 ^{bG}	3±0.4 ^{aA}	19.7±0.3 ^{aE}	30±1 ^{Ae}
	1.0	0	91.4±1 ^{aA}	4.2±0.1 ^{aA}	18.3±0.9 ^{aA}	29.7±0.8 ^{aA}
		24	104.6±0.5 ^{cF}	1.9±0.1 ^{bBC}	21.5±0.2 ^{bD}	31.1±0 ^{aD}
	2.0	0	93.7±1.3 ^{aA}	4.3±0.7 ^{aAB}	19.9±1.5 ^{aA}	29.3±0.6 ^{aA}
		24	109.4±0.4 ^{dF}	1.1±0.2 ^{cC}	23.3±0.3 ^{cB}	33.6±0.5 ^{bBC}
Cs-F	**0.5**	0	92.4±0.6 ^{aA}	3.9±0.3 ^{aAB}	18.4±0.6 ^{aA}	29.6±0.3 ^{aA}
		24	91.2±1.2 ^{aH}	2.9±0.3 ^{aA}	19.3±0.2 ^{cE}	29.5±0.9 ^{aF}
	1.0	0	92.2±0.2 ^{aA}	4.8±0.2 ^{aA}	18.5±1.1 ^{aA}	29.9±1.4 ^{aA}
		24	101.2±0.5 ^{bG}	2.1±0.2 ^{bB}	21.1±0.5 ^{bD}	29.7±1.2 ^{aF}
	2.0	0	91.2±0.9 ^{aA}	4.9±0.5 ^{aA}	18.9±0.9 ^{aA}	29.8±0.6 ^{aA}
		24	105±1.5 ^{cF}	1.4±0.3 ^{cC}	22.8±0.1 ^{cC}	32.9±0.3 ^{bC}
Cs-X	**0.5**	0	91.2±0.9 ^{aA}	4.1±0.8 ^{aAB}	19.9±1.5 ^{aA}	29.6±0.6 ^{aA}
		24	108.9±0.1 ^{bE}	2.3±0.1 ^{aB}	19.4±0 ^{aE}	29.5±0.2 ^{aF}
	1.0	0	92.8±0.2 ^{aA}	4.5±0.2 ^{aA}	18.3±1.2 ^{aA}	29.3±1.1 ^{aA}
		24	111.6±0.4 ^{cD}	1.6±0.4 ^{bBC}	22.4±0.1 ^{bC}	32.7±0.6 ^{bC}
	2.0	0	93.9±0.9 ^{aA}	4.2±0.4 ^{aAB}	18.9±0.2 ^{aA}	29.4±0.4 ^{aA}
		24	113.8±0.4 ^{dC}	1.4±0.3 ^{bC}	24.9±0.4 ^{cB}	34.8±0.3 ^{cB}
Cs-A	**0.5**	0	92.6±0.8 ^{aA}	4.6±0.2 ^{aA}	18.7±0.8 ^{aA}	29.1±0.7 ^{aA}
		24	109.2±0.4 ^{bE}	1.8±0.4 ^{aBC}	21.2±0.6 ^{aD}	32.1±1.1 ^{aC}
	1.0	0	91.4±0.6 ^{aA}	4.4±0.6 ^{aAB}	19.2±0.7 ^{aA}	29.8±0.6 ^{aA}
		24	115.2±1 ^{cB}	1.4±0.2 ^{aC}	23.8±0.2 ^{bB}	34.9±0.9 ^{bB}
	2.0	0	93.2±0.7 ^{aA}	4.6±0.1 ^{aA}	19±0.2 ^{aA}	30±0.4 ^{aA}
		24	118.4±1.5 ^{dA}	1.2±0.2 ^{aC}	26.7±0.8 ^{cA}	37.1±0.8 ^{cA}

362 Different letters (a-e) in the same films group are significantly different as determined by ANOVA test ($p<0.05$).
363 Different letters (A-H) indicated significant differences between different films groups at the same heating time ($p<0.05$).
364 **Cs:** Chitosan, **A:** Arabinose, **F:** Fructose, **G:** Glucose, **X:** Xylose.

No significant difference was shown regarding the WCA of non-heated films and for MR-treated Cs-fructose films at a mass ratio of 0.5% (w/w Cs), with an average WCA value of 92 ° ($p>0.05$). Subsequently, overall Cs-based films could be considered as hydrophobic films. Apart from that, as a result of Cs-saccharide MR crosslinking, WCA increased in a saccharide dose dependent manner ($p<0.05$), which could be attributed to the decrease in the hydrophilic character of heated films, as a result of polar groups decrease. For example, in the case of Cs-arabinose MR treated films, WCA values of 109 °, 115 ° and 118 ° were noted at mass ratios of 0.5, 1.0 and 2.0% (w/w Cs), respectively. As well, WCA increased from 100 ° to 109 ° and from 108 ° to 113 °, for Cs-xylose and Cs-glucose mass ratios of 0.5% and 2.0% (w/w Cs), respectively.

Taking into consideration these outcomes, the increase in films surface hydrophobicity, reflected by higher WCA values, was the most pronounced in the case of MR crosslinking with aldopentoses (arabinose and xylose), whereas, ketosis (fructose) was the less reactive, showing a relative crosslinking extent, after films heating at 90 °C for 24 h.

3.1.4. Water vapor permeability assessment

The effect of the MR crosslinking on the water barrier properties of Cs-based films was studied, considering films WVP (10^{-10} g m^{-1} s^{-1} Pa^{-1}) measured at 100% RH and results are summarized in **Table 1**. No significant differences in the WVP values were noted for the non-heated and heated free-saccharide Cs-based film, as well as non-heated saccharides-added films ($p>0.05$). However, WVP of heated films significantly decreased with the addition of saccharides to the film forming solutions, compared to the blank Cs-based film (3.4 10^{-10} g m^{-1} s^{-1} Pa^{-1}). This decrease was saccharide type and dose dependent, where films crosslinked with aldopentoses (less carbons in their macromolecular chain, with a carbonyl group at the end of the carbon chain) displayed the lowest WVP ($p<0.05$). Values of 1.4 10^{-10} g m^{-1} s^{-1} Pa^{-1} and 1.6 10^{-10} g m^{-1} s^{-1} Pa^{-1} were reached with 1.0% (w/w Cs) of arabinose and xylose, respectively. The

lowest reactivity, expressed in terms of the highest WVP value of 2.1 10^{-10} g m^{-1} s^{-1} Pa^{-1}, was observed with the Cs-fructose crosslinked films (ketosis), at the same concentration. Additionally, WVP decreased from 1.8 to 1.2 10^{-10} g m^{-1} s^{-1} Pa^{-1}, when the concentration of arabinose increased from 0.5 to 2.0% (w/w Cs). The same trend was noted with the xylose, fructose and glucose ($p<0.05$).

The decrease in the WVP could be ascribed to the reduction of the films network free volume (films pore size), subsequently to the MR crosslinking. This allowed a sufficient strengthening of the polymeric network, and thereby, the enhancement of Cs-MR-treated films mechanical properties. Therefore, a significant effect on the diffusion of water, among very small molecules (Hazaveh *et al*., 2015). Serrano-Leon *et al.* (2018) stated that the film barrier properties are affected by the filmogenic matrix moisture content. Indeed, a decrease in water concentration results in a decrease in molecular chains' mobility, ultimately changing permeability behavior of the MR-treated films.

3.2. Effect of the MR on films color and light barrier properties

3.2.1. Study of films color parameters

Optical features, including color, besides physicochemical and thermal behavior, are a key character to substantiate the effectiveness of packaging intended to food applications (Jiang *et al*., 2016). Visually, no significant modification was noted regarding non-heated blank and Cs-saccharides films color (**Supplementary Data Fig. S2**). Whereas, the color of MR crosslinked films shifted from colorless to dark yellow to variable extent, depending on the type and dose of incorporated saccharide. Therefore, changes in color of blank and MR-treated Cs-based films were determined and shown in **Table 2**. L* (whiteness/darkness), a* (redness/greenness) and b* (yellowness/blueness) values were used for the quantification of films color. Higher L*, negative a* and b* values imply lightness, green and blue color, respectively, while positive a* and b* values indicate red and yellow color, respectively.

In the present study, L* values decreased with the increase of saccharide content in the Cs-film forming solution, reaching a minimum of 85% in the presence of 2.0% (w/w Cs) of arabinose, after a 24 h heating time at 90 °C ($p<0.05$). Values of 88% and 87% were revealed with arabinose mass ratios of 0.5 and 1.0% (w/w Cs). While, negligible variations of lightness were detected for non-heated films and even for heated blank film ($p>0.05$), proving that color was not mainly affected by heating. The higher L* were displayed in the presence of fructose (ketosis), showing relative crosslinking rate, since the developpement of dark products is correlated with the extent of Cs-saccharide interaction through the MR. L* values of 90%, 89% and 88% were recorded for 0.5, 1.0 and 2.0% (w/w Cs) mass ratios of fructose. Lipid oxidation and food quality are mainly influenced by packaging material opacity, which is a key feature to substantiate the effectiveness of packaging intended to food applications as a protective agent of food materials from degradative effects of light. Indeed, light, specifically UV light, is mainly involved in the oxidation process, by chemical reactions catalyzation, which accelerates the deterioration of food, affecting ultimately its acceptability by the consumer (Su *et al*., 2012).

In addition, MR led to a significant intensification of Cs-based films dark yellowish color as illustrated by b* values measurements (**Table 2**). Indeed, b* increased significantly from 3.6 for blank Cs-based film to 10.9, 21.5, 25.7 and 31.6 for 2.0% (w/w Cs) content of fructose, glucose, xylose and arabinose, respectively. Even at the least mass ratio of 0.5% (w/w), a significant and rapid improvement in films yellowish color, by 2, 2.4, 2.6 and 3-folds, was observed for fructose, glucose, xylose and arabinose, respectively. In line with L* results, ketosis (fructose) was the least reactive, while aldopentoses (particularly arabinose) showed the highest MR crosslinking extent. A different tendency was noted regarding the a* coordinates, where values decreased toward the green region with MR crosslinking, depending on the saccharide type and dose (**Table 2**). Equally, no significant changes were detected for the non-heated films and the blank Cs-based film ($p>0.05$).

440 **Table 2:** Color parameters, browning index (BI) and transparency of Cs-based MR-
441 treated films, compared to the non-modified control film.

Film formulations		MR heating time (h)	Color parameters				BI	Transparency
			L*	a*	b*	ΔE		
Cs		0	91.2±0.4 ^{aA}	2.4±0.1 ^{aA}	3.6±0.3 ^{aA}	-	-	0.9±0.1 ^{aA}
		24	91.2±0.4 ^{aA}	2.4±0.1 ^{aA}	3.6±0.3 ^{aA}			1±0.1 ^{aA}
Cs-G	0.5	0	91.3±0.7 ^{aA}	2.4±0.2 ^{aA}	3.6±0.6 ^{aA}	-	-	0.9±0 ^{aA}
		24	89.1±0.1 ^{bC}	-0.9±0 ^{bB}	8.8±0.4 ^{bC}	5.9±1 ^{cBC}	9.3±0.5 ^{aC}	2.6±0.1 ^{bC}
	1.0	0	91.8±0.3 ^{aA}	2.3±0.1 ^{aA}	3.4±0.5 ^{aA}	-	-	0.9±0.1 ^{aA}
		24	88.5±0.1 ^{cC}	-1.4±0.1 ^{cC}	11.3±0.7 ^{cC}	9.1±0.6 ^{bC}	12±0.8 ^{bC}	3.8±0.1 ^{cD}
	2.0	0	91.2±0.4 ^{aA}	2.3±0.5 ^{aA}	3.5±0.2 ^{aA}	-	-	1±0.1 ^{aA}
		24	87.1±0.4 ^{dC}	-2.1±0 ^{dC}	21.5±1 ^{dC}	19±0.8 ^{aC}	25.5±1.3 ^{cC}	4±0 ^{dC}
Cs-F	0.5	0	91.3±0.5 ^{aA}	2.4±0.8 ^{aA}	3.6±0.3 ^{aA}	-	-	0.9±0.2 ^{aA}
		24	90.6±0.2 ^{bB}	-0.9±0.1 ^{bB}	7.5±0.4 ^{bB}	5.1±0.4 ^{cC}	7.6±0.4 ^{cD}	2.3±0.2 ^{bC}
	1.0	0	91.6±0.9 ^{aA}	2.5±0.1 ^{aA}	3.4±0.4 ^{aA}	-	-	0.9±0 ^{aA}
		24	89.5±0.2 ^{cB}	-1.2±0.1 ^{cB}	9.2±0.3 ^{cB}	7±0.3 ^{bD}	9.5±0.3 ^{bD}	3.5±0.1 ^{cC}
	2.0	0	90.9±0.6 ^{aA}	2.5±0.4 ^{aA}	3.5±0.7 ^{aA}	-	-	1±0.1 ^{aA}
		24	88.2±0.1 ^{dB}	-1.4±0.1 ^{dB}	10.9±0.6 ^{dB}	8.8±0.5 ^{aD}	11.5±0.7 ^{aD}	4±0.1 ^{dC}
Cs-X	0.5	0	91.3±0.8 ^{aA}	2.4±0.2 ^{aA}	3.6±0.3 ^{aA}	-	-	1±0.1 ^{aA}
		24	88.6±0.1 ^{bD}	-0.9±0 ^{bB}	9.4±0.3 ^{bC}	7.2±0.3 ^{cB}	10.1±0.3 ^{cB}	3±0 ^{bB}
	1.0	0	92±0.7 ^{aA}	2.4±0.1 ^{aA}	3.6±0.2 ^{aA}	-	-	1±0.1 ^{aA}
		24	87.2±0.1 ^{cD}	-2.7±0.1 ^{cD}	13±0.4 ^{cD}	11.5±0.4 ^{bB}	13.3±0.8 ^{bB}	4.7±0.1 ^{cB}
	2.0	0	92.1±0.9 ^{aA}	2.5±0.3 ^{aA}	3.6±0.1 ^{aA}	-	-	1±0 ^{aA}
		24	86.3±0.6 ^{dD}	-3.4±0.2 ^{dD}	25.7±0.4 ^{dD}	23.4±0.2 ^{aB}	30.9±0.6 ^{aB}	5.5±0 ^{dB}
Cs-A	0.5	0	91.3±0.9 ^{aA}	2.4±0.4 ^{aA}	3.6±0.1 ^{aA}	-	-	1±0.1 ^{aA}
		24	88.5±0.5 ^{bD}	-1.4±0.1 ^{bC}	11.1±0.3 ^{bD}	8.9±0.1 ^{cA}	11.7±0.3 ^{cA}	4±0.1 ^{bA}
	1.0	0	91.9±0.7 ^{aA}	2.4±0.3 ^{aA}	3.6±0.6 ^{aA}	-	-	1±0 ^{aA}
		24	87.2±0.3 ^{cE}	-2.8±0.2 ^{cD}	16.2±0.5 ^{cE}	14.3±0.6 ^{bA}	17.5±0.6 ^{bA}	5.2±0.1 ^{cA}
	2.0	0	92.2±0.5 ^{aA}	2.4±0.4 ^{aA}	3.7±0.4 ^{aA}	-	-	1.1±0 ^{aA}
		24	85.9±0.4 ^{dE}	-3.8±0.1 ^{dE}	31.6±0.5 ^{dE}	29.2±0.4 ^{aA}	40.6±0.5 ^{aA}	6.2±0.1 ^{dA}

442 Different letters (a-d) in the same films group are significantly different as determined by ANOVA test ($p<0.05$).
443 Different letters (A-E) indicated significant differences between different films groups at the same heating time ($p<0.05$).
444 **Cs:** Chitosan, **A:** Arabinose, **F:** Fructose, **G:** Glucose, **X:** Xylose.

To better study the above-mentioned differences between blank and MR-treated films, ΔE was determined (**Table 2**). Similarly, ΔE shapely increased with the increase of saccharide to Cs mass ratio, especially in the presence of aldopentoses, reaching values of 8.8, 19, 23 and 29 for fructose, glucose, xylose and arabinose, respectively ($p<0.05$).

Additionally, the BI, reflecting the extent of MR colored products developpement, was assessed. Results in **Table 2** show the BI variation of Cs-saccharide MR-conjugated films as a function of saccharide incorporated mass. Indeed, BI increased uniformly with the increase of saccharide content ($p<0.05$). For example, values reached more than 11, 17 and 40 for 0.5, 1.0 and 2.0% (w/w Cs) of arabinose, respectively. The highest BI values were noted in the presence of aldopentoses (xylose and especially arabinose), followed by glucose (aldohexoses). The lowest MR progress, in terms of the lowest BI values, was attained with fructose (ketosis), which is in line with ΔE and b values. Such findings proved that Cs-MR-conjugated films are dark with yellowish color, attributed to the developpement of MR colored products, which could result in an enhancement of their light barrier ability in the visible range.

Furthermore, it was found that the same trend of variation in terms of total color difference and water solubility was followed as a function of MR crosslinking extent (saccharide type and dose). In fact, the MR could be summarized as follows: at the early stage of the MR, conjugates (Schiff base) between the carbonyl group of saccharides and the amine group of Cs are formed, and subsequently cyclizes to develop the Amadori compounds. Thereafter, melanoidins, colored and insoluble polymeric compounds, are formed, allowing the noticeable drop of the Cs-MR-crosslinked films WS and the increase of their BI (Stevenson *et al*., 2020).

3.2.2. Light barrier properties assessment

Light, specifically UV light, is mainly implicated in the oxidation process, through chemical reactions catalyzation, hastening food deterioration, and thereby, its acceptability by

the consumer (Mahmoudi, Ostadhossein and Simchi, 2016). Therefore, UV and visible light transmission by Cs-MR-conjugated films was assessed in a wavelength range of 200–800 nm and compared with the blank Cs-based film behavior. Results, plotted in **Fig. 2**, reveal similar trends of variation as function of the MR extent with b*, ΔE and BI, ascribed to the progress of yellow-brown MR end products (melanoidins).

Blank Cs film exhibited a poor barrier property to the light in the UV range as observed through high transmission values at 280 and 350 nm, of 26.97% and 39.81%, respectively. Non-heated films, added with saccharides, showed no significant variations in the light barrier properties of the in terms of the transmittance values (**Fig. 2A-D**). In the range of 250–400 nm, Cs-MR-conjugated films spectra revealed particular absorption, in terms of light transmission values that decreased remarkably ($p<0.05$) (**Fig. 2E-H**). This is assumed to be ascribed to the light scattering or the interfering of light track, subsequently to Cs-saccharide crosslinking, hindering thereby light transmittance (Kaya *et al*., 2018). In fact, oxidation process mainly involves light, specifically UV light, which generates chemical reactions catalyzation, and accelerates the deterioration of food, affecting ultimately the consumer acceptance (Su *et al*., 2012).

The noteworthy light transmittance reduction at 280 nm, for Cs-MR-treated films reaching an average value of 1%, *vs.* 30% for blank Cs-based film, could be attributed to the presence of carbonyl compounds and heterocyclic derivatives (Etxabide *et al*., 2015). This remarkable UV light barrier increased concomitantly with the increase of saccharide to Cs mass ratio, indicating that Cs-MR-conjugated films effectively prevented UV light. The better barrier behavior, reflected by the lowest light transmittance values, was, as expected, observed with Cs crosslinked with aldopentoses (arabinose and xylose), indicating higher MR products developpement, compared to crosslinking with aldohexoses (glucose) and ketosis (fructose). The lower the transmittance value, the less transparent the films are (Souza *et al*., 2017).

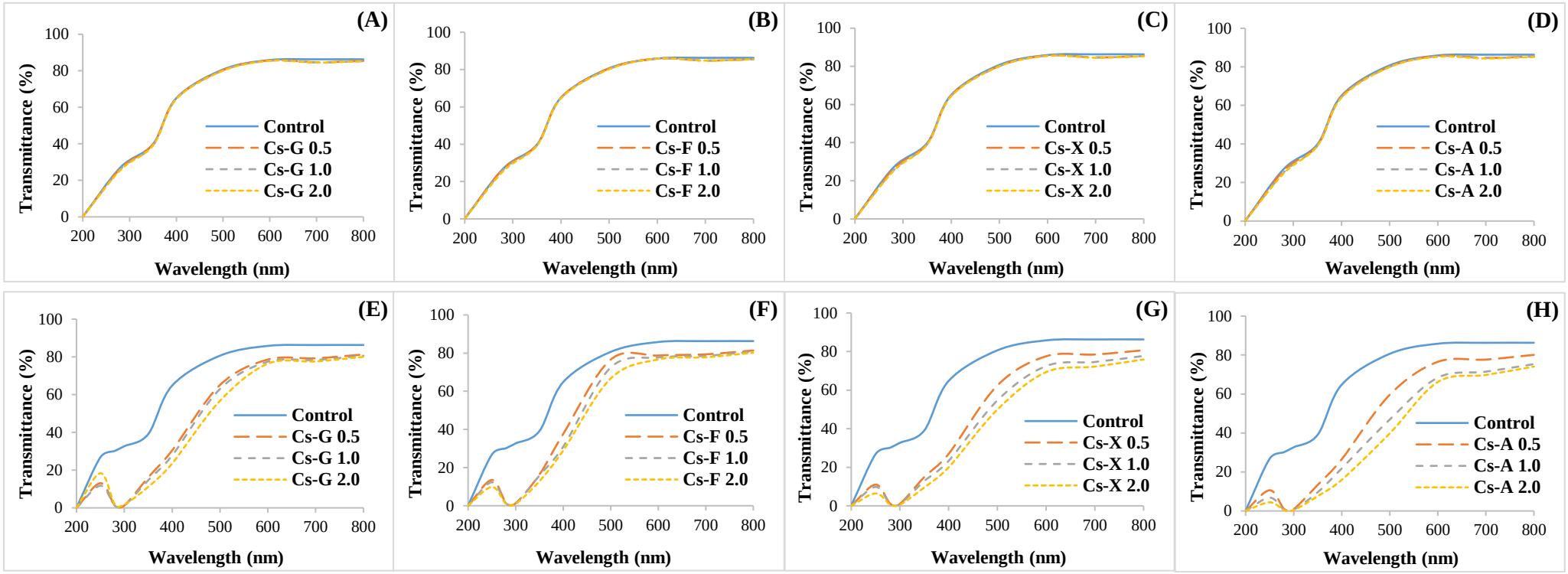

Figure 2: Transmittance of Cs-based films conjugated with different saccharides, at different mass ratios (0.5, 1.0 and 2.0 %; w/w Cs), through MR at 90 °C as a function of time (0 and 24 h). Non heated **(A-D)** and Heated **(E-H)** Cs-based films. **Cs:** Chitosan, **A:** Arabinose, **F:** Fructose, **G:** Glucose, **X:** Xylose.

Compared to the blank Cs-based film and Cs-saccharides non-heated films (average opacity of 0.9), the opacity values for the Cs-MR-crosslinked films were significantly higher ($p<0.05$), especially with aldopentoses (arabinose and xylose), indicating a lower transparency of the films (**Table 2**).

Cs-arabinose conjugated film at a mass ratio of 2.0% (w/w Cs) showed an enhancement in opacity by more than 6-folds, as compared to blank Cs-based film ($p<0.05$). This finding heightens the application of Cs-MR-conjugated films in food preservation (Stevenson *et al*., 2020; Mahmoudi, *et al*., 2016).

3.3. Infrared spectroscopic analysis

To further confirm the crosslinking in Cs-based films induced by the MR, besides chemical changes of Cs structure due to saccharide addition, FT-IR spectra of non-heated and heated Cs-saccharide films were studied and resulting patterns are shown in **Fig. 3**. Typical characteristic Cs absorption bands were revealed at around 1589 cm^{-1} attributed to N-H bending in the $NH\text{-}COCH_3$ group (amide II band), 1649 cm^{-1} characteristic of the amide I band (C=O in the $NHCOCH_3$ group), 1418 cm^{-1} indicating the C-H bending vibrations of CH_2, 2905 cm^{-1} ascribed as CH_2 and CH_3 groups, 894 cm^{-1} assigned to the absorption peaks of β-(1,4) glycosidic bands and at 3423 cm^{-1} attributed to the stretching vibrations of the OH and N-H groups (Hamdi *et al*., 2019b). additionally, for heated blank Cs-based film and non-heated Cs-saccharides films (**Fig. 3A-D**), no substantial modification of FT-IR spectra compared to the blank non-heated Cs-based film were detected. In addition, for all studied film samples, a glycerol characteristic band was detected at wavenumber 1046 cm^{-1}, which corresponded to the OH group vibrations (Vlacha *et al*., 2016).

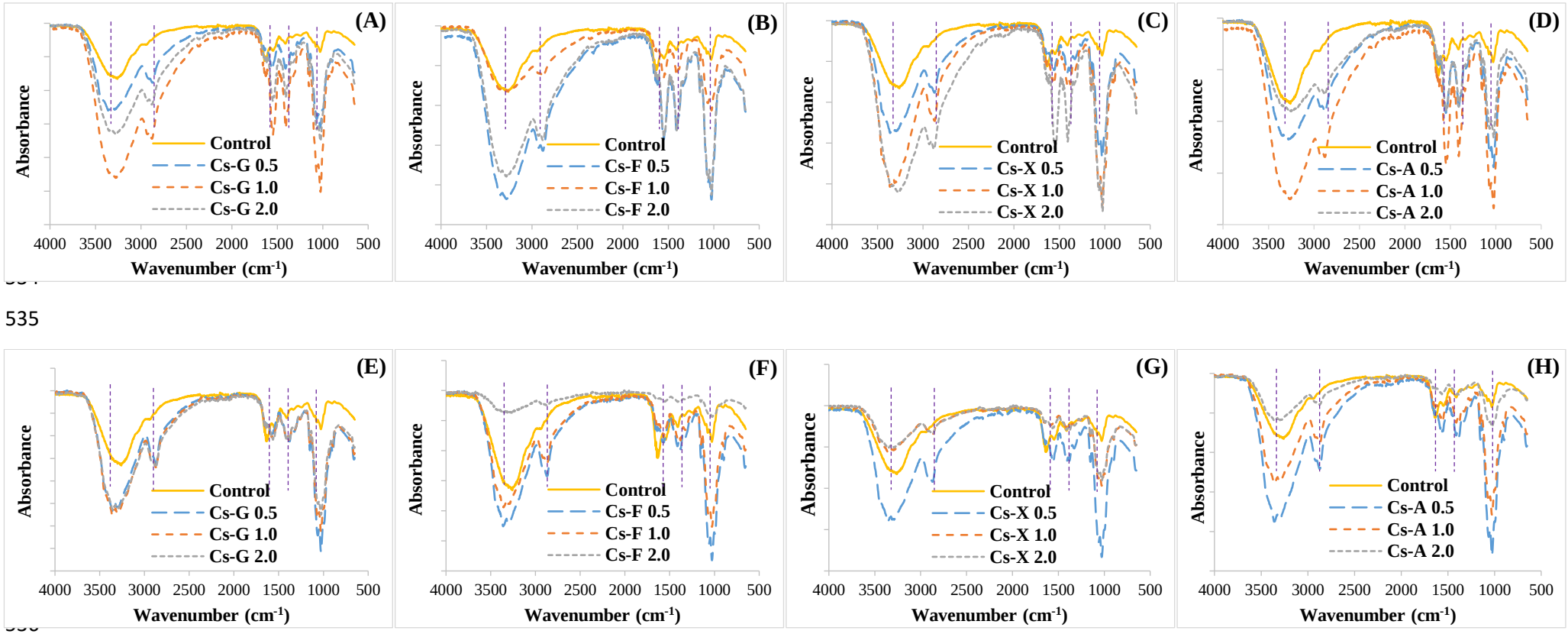

Figure 3: ATR -FTIR spectra of Cs-based films conjugated with different saccharides, at different mass ratios (0.5, 1.0 and 2.0 %; w/w Cs), through MR at 90 °C as a function of time (0 and 24 h). Non heated **(A-D)** and Heated **(E-H)** Cs-based films. **Cs:** Chitosan, **A:** Arabinose, **F:** Fructose, **G:** Glucose, **X:** Xylose.

The Cs and saccharides' intermolecular interactions were illustrated by the shifts in band positions (Stevenson *et al*., 2020; Xu *et al*., 2019; Ahmed and Ikram, 2016). Indeed, after reaction, independently of their type and concentration, saccharides addition to Cs caused significant difference in the resulting spectra (**Fig. 3E-H**). The absorption peak at wavenumber 1649 cm^{-1} (Amide I) decreased and shifted to 1607 cm^{-1} suggesting the formation of Schiff base (-C = N) between the saccharides reducing termination and the Cs amino groups (Zhong *et al*., 2019). In brief, the MR conjugation between an aldose sugar and an amino group of Cs stimulated the developpement of N-substituted glycosylamines that arranged to Amadori rearrangement products, the 1 amino-1-desoxy-2-ketoses. Thus, the formation of Schiff base of furfurals involved in aldols, aldimines, ketimes and melanoidins formation (Duconseille, Astruc, Quintana, Meersman and Sante-Lhoutellier, 2015).

Moreover, shifts from 1589 cm^{-1} (Amide II) to 1544 cm^{-1}, after 24 h MR time, were ascribed to the Cs conformation transformations, during the crosslinking reaction between Cs and saccharides. After MR crosslinking, more randomly disposition occurred, increasing, thereby, the molecular disorder (Badano *et al*., 2019). In fact, the reaction of the carbonyl group of each saccharide with the amino group of Cs, resulted in the elaboration of C-O-C ether linkage, due to -OH condensation. Therefore, overall change in Cs-saccharides glycated system took place and a characteristic adsorption in the wavenumber range of 1098-1021 cm^{-1} was detected (Du, Huang, Wang and Xiao, 2018).

3.4. Thermal behavior of Cs-based films as affected by the MR crosslinking

The thermal stability of Cs-based films crosslinked or not with the MR was assessed by TGA in a temperature range of 25 to 800 °C (**Supplementary Data Fig. S3**). The thermal decomposition data in terms of corresponding weight loss (Δw), temperature of maximum degradation (Tmax) and final residual mass (R) are reported in **Table 3**.

Table 3: Weight loss (Δw), temperature of maximum degradation (Tmax), residual mass (R) and glass transition temperature (Tg) of Cs-based films crosslinked with different saccharides of different molar ratios, *via* the MR at 90 °C.

Film formulations		MR heating time (h)	Δw (%)	Tmax (°C)	R (%)	Tg (°C)
Cs		0	67.2 ^{aA}	294.3 ^{aA}	25.9 ^{aA}	162.6 ^{aA}
		24	66.6 ^{bA}	292.8 ^{bA}	26.8 ^{aA}	169.9 ^{bA}
Cs-G	**0.5**	0	67.8 ^{aB}	296.7 ^{aC}	26 ^{aA}	162.4 ^{aA}
		24	66.8 ^{bA}	299.6 ^{cC}	30.2 ^{bB}	182.6 ^{cC}
	1.0	0	67.1 ^{aB}	297.9 ^{bD}	26.1 ^{aA}	163.2 ^{bA}
		24	66.3 ^{bA}	301.2 ^{dE}	30.6 ^{bB}	183.1 ^{dC}
	2.0	0	66.4 ^{bC}	299.2 ^{cF}	25.8 ^{aA}	162.9 ^{aA}
		24	65.9 ^{cB}	302 ^{eF}	31.4 ^{cB}	187.6 ^{eD}
Cs-F	**0.5**	0	69 ^{aA}	295.6 ^{aB}	25.9 ^{aA}	162.8 ^{aA}
		24	66.3 ^{cA}	298 ^{cB}	30.1 ^{bB}	179.1 ^{bB}
	1.0	0	67.1 ^{bB}	297.4 ^{bD}	26.1 ^{aA}	162.5 ^{aA}
		24	65.8 ^{dB}	298.9 ^{cdB}	30.6 ^{bB}	181.1 ^{cB}
	2.0	0	66.2 ^{cC}	298.8 ^{cdE}	26.1 ^{aA}	162.1 ^{aA}
		24	65.6 ^{dB}	300.4 ^{dD}	31.2 ^{bB}	184.6 ^{dB}
Cs-X	**0.5**	0	67.4 ^{aB}	298 ^{aE}	26.1 ^{aA}	162.3 ^{aA}
		24	66.3 ^{bA}	299.6 ^{bcC}	30.4 ^{bB}	183.4 ^{bD}
	1.0	0	67.4 ^{aB}	299.7 ^{bcF}	26 ^{aA}	162.9 ^{aA}
		24	66.3 ^{bA}	301.2 ^{dE}	31.5 ^{cC}	186.7 ^{cE}
	2.0	0	66.5 ^{bC}	300.4 ^{cG}	26.1 ^{aA}	162.7 ^{aA}
		24	65.1 ^{cB}	302.8 ^{eF}	32.2 ^{dC}	188.4 ^{dC}
Cs-A	**0.5**	0	67.6 ^{aB}	299.3 ^{aF}	25.9 ^{aA}	162.6 ^{aA}
		24	66.5 ^{bA}	300.4 ^{bD}	30.6 ^{bB}	183.9 ^{cD}
	1.0	0	66.4 ^{bC}	301.2 ^{cH}	26.1 ^{aA}	163.2 ^{bB}
		24	65.7 ^{cB}	302.1 ^{dE}	31.9 ^{cC}	185.8 ^{dD}
	2.0	0	64.9 ^{dD}	301.9 ^{cdH}	26.2 ^{aA}	163.1 ^{bB}
		24	63.8 ^{eC}	303.6 ^{eG}	32.8 ^{dC}	193.1 ^{eE}

Different letters (a-e) in the same films group are significantly different as determined by ANOVA test ($p<0.05$).
Different letters (A-H) indicated significant differences between different films groups at the same heating time ($p<0.05$). **Cs:** Chitosan, **A:** Arabinose, **F:** Fructose, **G:** Glucose, **X:** Xylose; **Tmax:** Temperature of the maximum degradation of the major transformation region; **R:** Residue.

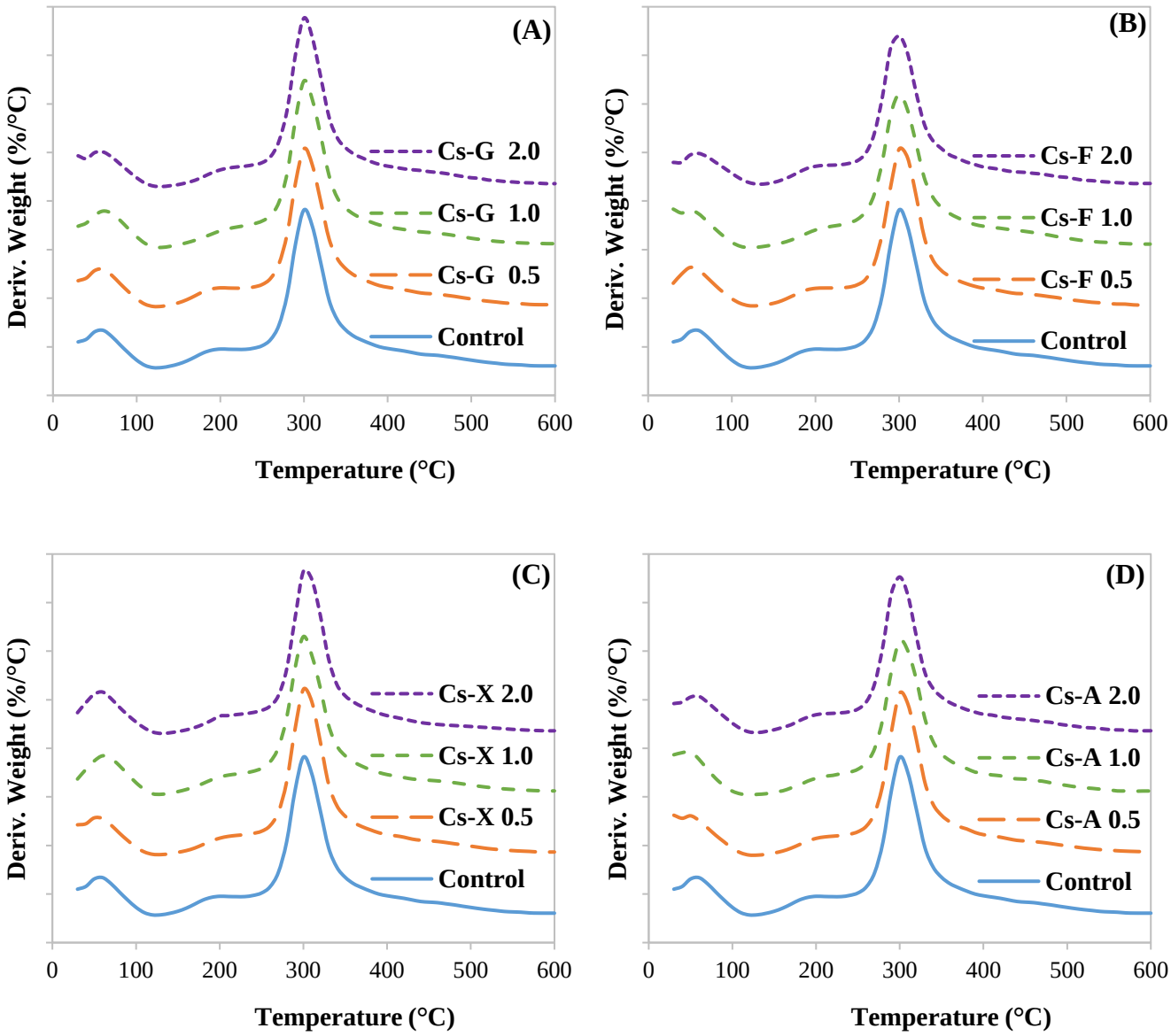

<u>Figure 4:</u> DTG profiles of Cs-based films conjugated with different saccharides, at different mass ratios (0.5, 1.0 and 2.0 %; w/w Cs), through MR at 90 °C for 24 h. **Cs:** Chitosan, **A:** Arabinose, **F:** Fructose, **G:** Glucose, **X:** Xylose.

Based on data from the obtained TGA thermograms, the thermal decomposition profiles of the overall films exhibited a similar weight loss process in the temperature range of 25 to 800 °C, characterized by two distinguishable major phases (**Fig. 4**), characteristic of chitosan-based biomaterials thermal decomposition. The first stage of transformation is related to the loss of free and bound water (below 100 °C), which tended to decrease for Cs-MR-crosslinked films, in line with the WC findings (**Fig. 1A**), proving that MR-treated films (90 °C, 24 h)

585 exhibited lower WC than the non-heated films. The second stage of weight loss, corresponding
586 to the major Δw around 63 to 67%, displayed the degradation or the decomposition of Cs chains
587 at approximately 292-303 °C.

588 Results in **Table 3** display that the incorporation of saccharides in the Cs film-forming
589 matrix without heat treatment did not affect significantly the Δw of films, at around 67%.
590 Nevertheless, the lowest Δw value was around 63% for Cs-arabinose crosslinked film, at a mass
591 ratio of 2.0% (w/w Cs).

592 Regarding Tmax values, no significant changes were noted for the non-heated films
593 ($p>0.05$). However, when comparing to the blank heated Cs-based film (292 °C), saccharides
594 incorporation increased Tmax values of Cs-MR-conjugated films in a saccharide dose
595 dependent manner ($p<0.05$), to reach by 300.4 °C, 302 °C, 302.8 °C and 303.6 °C for Cs-
596 fructose, Cs-glucose, Cs-xylose and Cs-arabinose crosslinked films, at a saccharide to Cs mass
597 ratio of 2.0% (w/w Cs), respectively (**Table 3**).

598 Similar trends were observed for the R values, which raised concomitantly with the
599 saccharide concentration, attaining a maximum R value of 32% with 2.0% (w/w Cs) of
600 aldopentoses (arabinose). This thermal resistance behavior could be correlated to the MR
601 crosslinking extent, through creation of new bonds between Cs macromolecular chains,
602 inducing their thermal stability. Additionally, MR products could interact with the Cs polymeric
603 matrix, allowing the stabilization of film network, thus the increase in the observed thermal
604 stability for Cs-MR-treated films (Kchaou *et al*., 2018; Su *et al*., 2012).

605 The thermal properties of Cs-MR-conjugated films were further assessed by the DSC
606 analysis in order to determine the glass transition temperature (Tg) and obtained results are
607 shown in **Table 3**. In the same line with TGA outcomes, a clear increase in all films Tg values
608 was displayed with increasing the saccharide content, which could be ascribed either to WC
609 decrease, or to crosslinking phenomenon. Indeed, the Tg increased from 169 °C for blank Cs-

based film to 184, 187, 188 and 193 °C for Cs-fructose, Cs-glucose, Cs-xylose and Cs-arabinose crosslinked films, at a saccharide to Cs mass ratio of 2.0% (w/w Cs), respectively ($p<0.05$). Even at low saccharide content of 0.5% (w/w Cs), improved Tg values of 179, 182, 183.4 and 183.9 °C for Cs-fructose, Cs-glucose, Cs-xylose and Cs-arabinose crosslinked films, respectively ($p<0.05$). Advantageously, DSC thermograms (**Supplementary Data Fig. S4**) reveal a single Tg for all the tested films indicating a good compatibility between tested saccharides and Cs, in these conditions (Hamdi *et al*., 2019a).

Consequently, the Tg as well as the degradation temperature enhancement approved that MR, through its crosslinking effect between the amino group of the glucosamine unit and the carbonyl of saccharide, modified the Cs polymeric structure, elaborating a more thermally stable matrix. This phenomenon is more pronounced in the presence of pentoses (arabinose and xylose), with less carbons in their macromolecular chain, showing higher crosslinking extent, resulting in higher degradation temperatures values, compared to the hexoses (fructose and glucose), with more carbons. Particularly, aldoses (arabinose, xylose and glucose), with a carbonyl group located at one end of the carbon chain, were more reactive than ketoses (fructose), with a carbonyl group situated inside the carbon chain. This enhanced and interesting thermal behavior of Cs-MR-conjugated films could be promising for upgraded mechanical properties.

3.5. Mechanical properties changes of Cs-based MR-treated films

To have information about their flexibility and stretchability, mechanical properties of Cs-saccharides crosslinked through the MR, in terms of TS and EAB were measured and compared to Cs-based film (**Table 1**). Indeed, used or predicted materials for food packaging need to uphold their integrity and effectively resist to plenty types of stress occurring during distribution, treatment and storage (Kaya *et al.*, 2018). Based on the tensile stress *vs.* strain curves, no significant effect of the addition of saccharides without heating, i.e. no MR occurred,

on the control films TS and EAB values was observed ($p>0.05$). In addition, heat treatment (90 °C for 24 h) did not affect the mechanical parameters of Cs-blank film ($p>0.05$).

In counterpart, subsequently to the MR crosslinking, a significant improvement of Cs-saccharides MR crosslinked films mechanical behavior was detected, considering the resultant increase of TS and EAB values, in a saccharide dose-dependent manner ($p<0.05$). In fact, TS values enhanced by 1.17, 1.28 and 1.45-folds, for 0.5, 1.0 and 2.0% (w/w Cs) of arabinose, compared to the blank Cs-based film (18.7 MPa). Equally, EAB increased from 29.8% for blank Cs-based film to 32.1% and 37.1% for 0.5% and 1.0% (w/w Cs) Cs-arabinose crosslinked films, respectively (**Table 1**). The same trend was noted for the other tested saccharides, but in the following order of reactivity: arabinose > xylose > glucose > fructose. The lowest TS value of 22.8 MPa and EAB of 32.9% were exhibited by the 2.0% (w/w Cs) Cs-fructose MR crosslinked film.

These advantageous mechanical properties of Cs-saccharides MR crosslinked films, particularly through conjugation with aldopentoses, among which arabinose and xylose, is in line with thermal (DSC and TGA) outcomes, proving a positive correlation between TS and Tg of films. Actually, the changes of Tg is not only a current indicator of additives and macromolecules compatibility in the film polymeric network, but it permits likewise to enlighten the polymeric material mechanical resistance parameters (Mujeeb Rahman, Abdul Mujeeb, Muraleedharan and Thomas, 2018). This particular behavior (more reactivity with aldopentoses than ketoses and hexoses) corroborated, as well, with the above described MC results, attributed to MR crosslinking, besides the saccharides plasticizing action (Kamboj *et al*., 2015).

3.6. Effect of the MR crosslinking on the microstructure of Cs-based films

The Cs-based films treated with the MR were analyzed for transverse sections after gold coating, to qualitatively visualize their microstructure (homogeneity, layer, voids, etc.) and to

identify microstructural modifications, allowing a better understanding of polymers film-forming behavior.

Based on the overall above reported results, the Cs-saccharides films at a concentration of 2.0% (w/w Cs) crosslinked through the MR (90 °C for 24 h) were selected for the SEM analysis, and compared with the non-added Cs-based film **(Fig. 5)**.

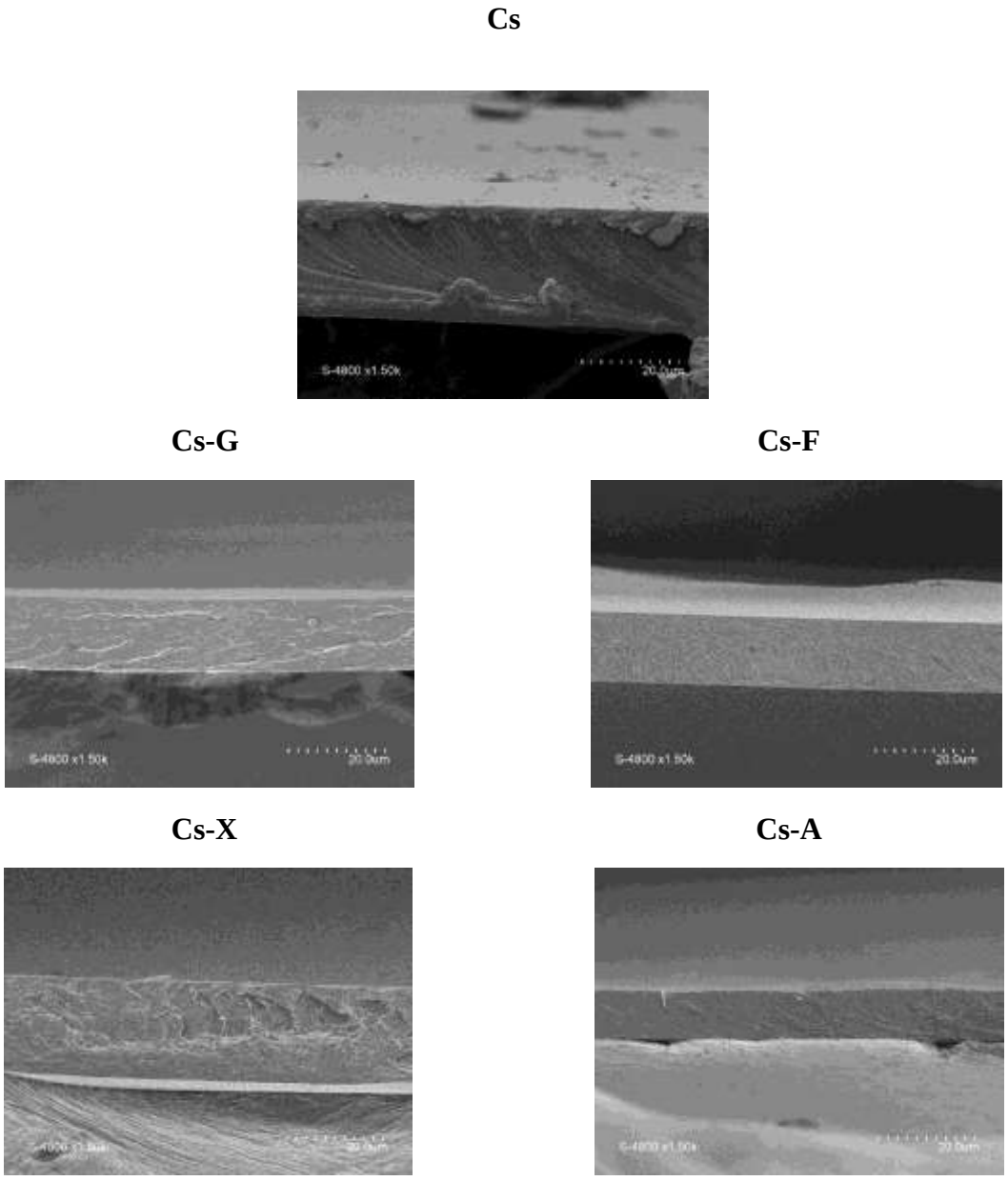

Figure 5: SEM cross-section (1.50 kV, 20 μm and 25.0 kV) of Cs-based films conjugated with different saccharides, at different mass ratios (0.5, 1.0 and 2.0 %; w/w Cs), through MR at 90 °C for 24 h. **Cs:** Chitosan, **A:** Arabinose, **F:** Fructose, **G:** Glucose, **X:** Xylose.

Characteristic micrographs of films cross-sections of films are shown in **Fig. 5**, where, a continuous, homogeneous phase in Cs-based film could be observed, without any evidence of irregularities (air bubbles, pores, cracks or droplets) or phase separation (Hamdi *et al*., 2019a).

The incorporation of saccharides into Cs network combined with heat treatment at 90 °C for 24 h distinguishably changed the cross-section structure of MR-treated films. It was possible to confirm more homogeneity and density were detected with higher crosslinking rates. Otherwise, aldopentoses (xylose and particularly arabinose) were more reactive toward the MR than ketosis (fructose) and aldohexoses (glucose), allowing higher rates of crosslinking, resulting in such peculiar microstructural arrangements. These film-forming ultra-structures are in agreement with FT-IR analysis, confirming the above observed results, in terms of thermal, mechanical and barrier behaviors (Mujeeb Rahman *et al*., 2018; Rubentheren *et al*., 2016).

3.7. Antioxidant activities of Cs-based MR crosslinked films

The global antioxidative mechanism could be ascribed to the cooperative effects of different systems, such as metal chelation and radicals scavenging (Zhang, Chen, Zhang, Ma and Xu, 2013). Therefore, to investigate the antioxidativity of the Cs-based MR crosslinked films, differents *in vitro* antioxidant tests were implemented: DPPH radical scavenging (free radicals quenching), reducing power (iron reduction ability) and metal chelating assays (**Fig. 6**). Data in the present work reveal that for all antioxidant systems investigated, values were remarkably higher ($p<0.05$) in Cs-based MR crosslinked films than in the blank Cs-based film. Indeed, blank Cs-based film exhibited weak reducing power of OD_{700}=0,165 ± 0009 (**Fig. 6A**), whereas, good antioxidant activities of 74.1 ± 0.58% and 75.27 ± 1.91% were displayed for DPPH radical scavenging (**Fig. 6B**) and metal chelating (**Fig. 6C**). The availability of -OH and -NH_2 groups throughout the polymer matrix reflected the antioxidant ability of Cs, thus Cs-based films antioxidant patterns (Badano *et al*., 2019; Hamdi *et al*., 2019a).

Subsequently to the MR crosslinking and the incorporation of saccharides into the film-forming matrix, the antioxidant activity was enhanced and values increased and was directly correlated to the amount of added saccharide. Interestingly, the reducing power antioxidant activity of Cs-based MR treated film with 0.5% and 2.0% of arabinose (w/w Cs) increased by more than 13- and 16-folds, respectively, compared to the blank Cs-based film (**Fig. 6A**). Moreover, the highest values of inhibition of 100% for DPPH radical scavenging (**Fig. 6B**) and metal chelating (**Fig. 6C**) were exhibited, at the same concentration of arabinose. Several mechanisms could be implicated in the antioxidant activity of Cs-based MR-treated films. Indeed, the reducing power could be attributed either to MR products formed in the primary phase of the MR during thermolysis of Amadori compounds, or to MR final stage heterocyclic compounds (Chen *et al*., 2019). Furthermore, the marked increase in the scavenging activity of MR-treated films could be associated with the reduction of the number of reactive amino groups produced by the MR, otherwise, the intermediates and the final brown polymer (melanoidins) could behave as hydrogen donors (Akar, Küçük and Doğan, 2017; Zhang, Shen, Zhu and Xu, 2015).

In line with above-mentioned in the FT-IR analysis and perceived by SEM, these findings could explain the fact that the extent of the MR, as reflected by higher in vitro antioxidant activities, was influenced by the type of saccharides ($p<0.05$). Pentoses (arabinose and xylose), with less carbons in their macromolecular chain, showed higher reducing power (**Fig. 6A**), radical scavenging (**Fig. 6B**) and metal chelating activities (**Fig. 6C**), compared to the hexoses (fructose and glucose), with more carbons. More particularly, aldoses (arabinose, xylose and glucose), with a carbonyl group located at one end of the carbon chain, were more reactive than ketosis (fructose), with a carbonyl group situated inside the carbon chain, which could be the result of higher covalent crosslinking extent.

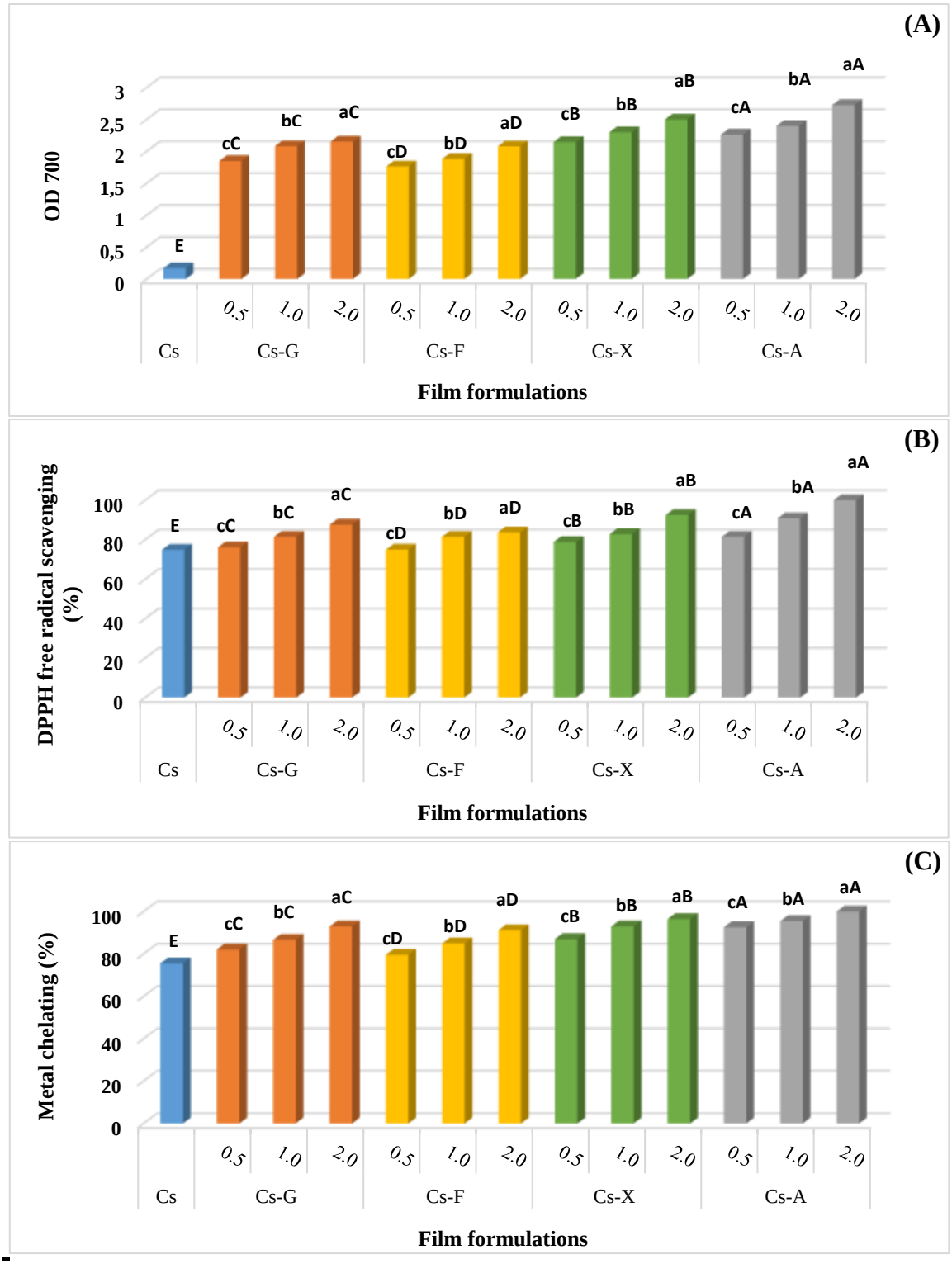

Figure 6: Antioxidant activities of Cs-based films conjugated with different saccharides, at different mass ratios (0.5, 1.0 and 2.0 %; w/w Cs), through MR at 90 °C for 24 h, based on the reducing power **(A)**, DPPH free radical scavenging **(B)** and metal chelation **(C)** *in vitro* tests. **Cs:** Chitosan, **A:** Arabinose, **F:** Fructose, **G:** Glucose, **X:** Xylose. Different letters $^{(a-c)}$ in the same films group are significantly different as determined by ANOVA test ($p<0.05$). Different letters $^{(A-D)}$ indicated significant differences between different films groups ($p<0.05$).

4. Conclusion

In the present work, different types of saccharides were incorporated at different mass ratios into chitosan film forming solution. Maillard reaction crosslinking was induced by films heating at 90 °C during 24 h. Advantageously, Maillard reaction increased water barrier and resistance of resulted films, as reflected by water solubility, water contact angle and water vapor permeability, in a saccharide type and dose-dependent manner. Treated films crosslinked with aldopentoses were, additionally, less transparent with enhanced light barrier than ketoses-treated films. Moreover, Maillard reaction allowed an improvement of the thermal resistance (in terms of glass transition and degradation temperatures) and mechanical behavior, compared to blank non-treated film. Furthermore, Maillard reactions could be considered as an alternative tool to develop chitosan-based films with improved antioxidativity that could then be used as active packaging against foods oxidation, especially using aldopentoses as crosslinkers. The subsequent application of the prepared films in the packaging of food samples, such as oil, fish fillet, etc., is of great interest to concretely confirm their effectiveness.

Acknowledgements

The present work was funded by the Ministry of Higher Education and Scientific Research, Tunisia. The authors gratefully acknowledge Dr. Christophe CHARMETTE for his helpful aid regarding the water vapor permeability measurements and Dr. Thierry THAMI for water contact angles analyses.

References

Ahmed, S., Ikram, S. (2016). Chitosan and gelatin based biodegradable packaging films with UV-light protection. *Journal of Photochemistry and Photobiology B: Biology*, **163**, 115-124.

Akar, Z., Küçük, M., Doğan, H. (2017). A new colorimetric DPPH• scavenging activity method with no need for a spectrophotometer applied on synthetic and natural antioxidants and medicinal herbs. *Journal of Enzyme Inhibition and Medicinal Chemistry*, **32**, 640-647.

Akyuz, L., Kaya, M., Koc, B., Mujtaba, M., Ilk, S., Labidi, J., Salaberria, A.M., Cakmak, Y.S., Yildiz, A. (2017). Diatomite as a novel composite ingredient for chitosan film with enhanced physicochemical properties. *International Journal of Biological Macromolecules*, **105**, 1401-1411.

Al Jahwari, F., Pervez, T. (2019). The potential of environmental-friendly biopolymers as an alternative to conventional petroleum-based polymers. *Reference Module in Materials Science and Materials Engineering* https://doi.org/10.1016/B978-0-12-803581-8.11295-0

Assadpour, E., Jafari, S.M. (2019). Chapter 3 - Nanoencapsulation: Techniques and Developments for Food Applications. In: Rubio, A.M., Sanz, M.M., Rovira, M.J.F., Gómez-Mascaraque, L.G. (Eds.), *Nanomaterials for Food Applications-Micro and Nano Technologies* (pp. 35-61). Elsevier Inc.

Badano, J.A., Braber, N.V., Rossi, Y., Diaz Vergara, L., Bohl, L., Porporatto, C., Falcone, R.D., Montenegro, M. (2019). Physicochemical, *in vitro* antioxidant and cytotoxic properties of water-soluble chitosan-lactose derivatives. *Carbohydrate Polymers*, **224**, 115158.

Bersuder, P., Hole, M., Smith, G. (1998). Antioxidants from a heated histidine-glucose model system. I: Investigation of the antioxidant role of histidine and isolation of antioxidants by high-performance liquid chromatography. *Journal of the American Oil Chemists' Society*, **75**, 181–187.

Cai, L., Li, D., Dong, Z., Cao, A., Lin, H., Li, J. (2016). Change regularity of the characteristics of Maillard reaction products derived from xylose and Chinese shrimp waste hydrolysates. *LWT - Food Science and Technology*, **65**, 908-916.

Chen, K., Yang, X., Huang, Z., Jia, S., Zhang, Y., Shi, J., Hong, H., Feng, L., Liu, Y. (2019). Modification of gelatin hydrolysates from grass carp (*Ctenopharyngodon idellus*) scales by Maillard reaction: Antioxidant activity and volatile compounds. *Food Chemistry*, **295**, 569-578.

Debeaufort, F., Martin-Polo, M., Voilley, A. (1993). Polarity homogeneity and structure affect water vapor permeability of model edible films. *Journal of Food Science*, **58**, 426-429.

Decker, E.A., Welch, B. (1990). Role of ferritin as a lipid oxidation catalyst in muscle food. *Journal of Agricultural and Food Chemistry*, **38**, 674–677.

Du, Y.L., Huang, G.Q., Wang, H.O., Xiao, J.X. (2018). Effect of high coacervation temperature on the physicochemical properties of resultant microcapsules through induction of Maillard reaction between soybean protein isolate and chitosan. *Journal of Food Engineering*, **234**, 91-97.

Duconseille, A., Astruc, T., Quintana, N., Meersman, F., Sante-Lhoutellier, V. (2015). Gelatin structure and composition linked to hard capsule dissolution: A review. *Food Hydrocolloids*, **43**, 360-376.

Etxabide, A., Urdanpilleta, M., Guerrero, P., de la Caba, K. (2015). Effects of crosslinking in nanostructure and physicochemical properties of fish gelatins for bio-applications. *Reactive and Functional Polymers*, **94**, 55-62.

Fernandez-de Castro, L., Mengíbar M., Sanchez, A., Arroyo, L., Villaran, M.C., Díaz de Apodaca, E., Heras, A. (2016). Films of chitosan and chitosan-oligosaccharide neutralized and thermally treated: Effects on its antibacterial and other activities. *LWT - Food Science and Technology*, **73**, 368-374.

Galiano, F., Briceño, K., Marino, T., Molino, A., Christensen, K.V., Figoli, A. (2018). Advances in biopolymer-based membrane preparation and applications. *Journal of Membrane Science*, **564**, 562-586.

Gennadios, A., Handa, A., Froning, G.W., Weller, C.L., Hanna, M.A. (1998). Physical properties of egg white-dialdehyde starch films. *Journal of Agricultural and Food Chemistry*, **46**, 1297–1302.

808 Gullon, B., Montenegro, M.I., Ruiz-Matute, A.I., Cardelle-Cobas, A., Corzo, N., Pintado, M.E.
809 (2016). Synthesis, optimization and structural characterization of a chitosan–glucose
810 derivative obtained by the Maillard reaction. *Carbohydrate Polymers*, **137**, 382-389.
811 Hamdi, M., Hajji, S., Affes, S., Taktak, W., Maâlej, H., Nasri, M., Nasri, R. (2018).
812 Development of a controlled bioconversion process for the recovery of chitosan from blue
813 crab (*Portunus segnis*) exoskeleton. *Food Hydrocolloids*, **77**, 534-548.
814 Hamdi, M., Nasri, R., Li, S., Nasri, M. (2019a). Bioactive composite films with chitosan and
815 carotenoproteins extract from blue crab shells: Biological potential and structural,
816 thermal, and mechanical characterization. *Food Hydrocolloids*, **89**, 802–812.
817 Hamdi, M., Nasri, R., Hajji, S., Nigen, M., Li, S., Nasri, M. (2019b). Acetylation degree, a key
818 parameter modulating chitosan rheological, thermal and film-forming properties. *Food*
819 *Hydrocolloids*, **87**, 48-60.
820 Hazaveh, P., Mohammadi Nafchi, A., Abbaspour, H. (2015). The effects of sugars on moisture
821 sorption isotherm and functional properties of cold-water fish gelatin films. *International*
822 *Journal of Biological Macromolecules*, **79**, 370-376.
823 Jiang, S., Zhang, X., Ma, Y., Tuo, Y., Qian, F., Fu, W., Mu, G. (2016). Characterization of
824 whey protein-carboxymethylated chitosan composite films with and without
825 transglutaminase treatment. *Carbohydrate Polymers*, **153**, 153–159.
826 Joye, I.J. (2019). Cereal biopolymers for nano- and microtechnology: A myriad of opportunities
827 for novel (functional) food applications. *Trends in Food Science & Technology*, **83**, 1-11.
828 Kamboj, S., Singh, K., Tiwary, A.K., Rana, V. (2015). Optimization of microwave assisted
829 Maillard reaction to fabricate and evaluate corn fiber gum-chitosan IPN films. *Food*
830 *Hydrocolloids*, **44**, 260-276.
831 Kaya, M., Ravikumar, P., Ilk, S., Mujtaba, M., Akyuz, L., Labidi, J., Salaberria, A.M., Cakmak,
832 Y.S., Erkul, S.K. (2018). Production and characterization of chitosan based edible films
833 from *Berberis crataegina*'s fruit extract and seed oil. *Innovative Food Science &*
834 *Emerging Technologies*, **45**, 287–297.
835 Kchaou, H., Benbettaïeb, N., Jridi, M., Abdelhedi, O., Karbowiak, T., Brachais, C.H., Léonard,
836 M.L., Debeaufort, F., Nasri, M. (2018). Enhancement of structural, functional and
837 antioxidant properties of fish gelatin films using Maillard reactions. *Food Hydrocolloids*,
838 **83**, 326-339.
839 Lakshmi Kosaraju, S., Weerakkody, R., Augustin, M.A. (2010). Chitosan-glucose conjugates:
840 influence of extent of Maillard reaction on antioxidant properties. *Journal of Agricultural*
841 *and Food Chemistry*, **58**, 12449-12455.
842 Leceta, I., Guerrero, P., Ibarburu, I., Dueñas, M.T., de la Caba, K. (2013). Characterization and
843 antimicrobial analysis of chitosan-based films. *Journal of Food Engineering*, **116**, 889–
844 899.
845 Liu, J., Sun, L., Xu, W., Wang, Q., Yu, S., Sun, J. (2019). Current advances and future
846 perspectives of 3D printing natural-derived biopolymers. *Carbohydrate Polymers*, **207**,
847 297-316.
848 Mahmoudi, N., Ostadhossein, F., Simchi, A. (2016). Physicochemical and antibacterial
849 properties of chitosan-polyvinylpyrrolidone films containing self-organized graphene
850 oxide nanolayers. *Journal of Applied Polymer Science*, **133**, 43194.
851 Matiacevich, S.B., Pilar Buera, M. (2006). A critical evaluation of fluorescence as a potential
852 marker for the Maillard reaction. *Food Chemistry*, **95**, 423-430.
853 Mujeeb Rahman, P., Abdul Mujeeb, V.M., Muraleedharan, K., Thomas, S.K. (2018).
854 Chitosan/nano ZnO composite films: Enhanced mechanical, antimicrobial and dielectric
855 properties. *Arabian Journal of Chemistry*, **11**, 120–127.

856 Mujtaba, M., Morsi, R.E., Kerch, G., Elsabee, M.Z., Kaya, M., Labidi, J., Khawar, K.M. (2019).
857 Current advancements in chitosan-based film production for food technology; A review.
858 *International Journal of Biological Macromolecules*, **121**, 889-904.
859 Park, S.B., Lih, E., Park, K.S., Joung, Y.K., Han, D.K. (2017). Biopolymer-based functional
860 composites for medical applications. *Progress in Polymer Science*, **68**, 77-105.
861 Prameela, K., Mohan, C.M., Ramakrishna, C. (2018). Chapter 1 - Biopolymers for Food
862 Design: Consumer-Friendly Natural Ingredients. In: Grumezescu, A.M. (Eds.),
863 *Biopolymers for Food Design-Handbook of Food Bioengineering* (pp. 1-32). Elsevier Inc.
864 Rubentheren, V., Ward, T.A., Chee, C.Y., Nair, P., Salami, E., Fearday, C. (2016). Effects of
865 heat treatment on chitosan nanocomposite film reinforced with nanocrystalline cellulose
866 and tannic acid. *Carbohydrate Polymers*, **140**, 202-208.
867 Rui, L., Xie, M., Hu, B., Zhou, L., Yin, D., Zeng, X. (2017). A comparative study on
868 chitosan/gelatin composite films with conjugated or incorporated gallic acid.
869 *Carbohydrate Polymers*, **173**, 473–481.
870 Serrano-Leon, J.S., Bergamaschi, K.B., Yoshida, C.M.P., Saldana, E., Selani, M.M., Rios-
871 Mera, J.D., Alencar, S.M., Contreras-Castillo, C.J. (2018). Chitosan active films
872 containing agro-industrial residue extracts for shelf life extension of chicken restructured
873 product. *Food Research International*, **108**, 93-100.
874 Shariatinia, Z. (2018). Carboxymethyl chitosan: Properties and biomedical applications.
875 *International Journal of Biological Macromolecules*, **120**, 1406–1419.
876 Souza, V.G.L., Fernando, A.L., Pires, J.R.A., Rodrigues, P.F., Lopes, A.A.S., Braz Fernandes,
877 F.M. (2017). Physical properties of chitosan films incorporated with natural antioxidants.
878 *Industrial Crops & Products*, **107**, 565-572.
879 Stevenson, M., Long, J., Seyfoddin, A., Guerrero, P., de la Caba, K., Etxabide, A. (2020).
880 Characterization of ribose-induced crosslinking extension in gelatin films. *Food*
881 *Hydrocolloids*, **99**, 105324.
882 Su, J.F., Yuan, X.Y., Huang, Z., Wang, X.Y., Lu, X.Z., Zhang, L.D., Wang, S.B. (2012).
883 Physicochemical properties of soy protein isolate/carboxymethyl cellulose blend films
884 crosslinked by Maillard reactions: Color, transparency and heat-sealing ability. *Materials*
885 *Science and Engineering: C*, **32**, 40-46.
886 Sung, W.C., Chang, Y.W., Chou, Y.H., Hsiao, H. (2018). The functional properties of chitosan-
887 glucose-asparagine Maillard reaction products and mitigation of acrylamide formation by
888 chitosans. *Food Chemistry*, **243**, 141-144.
889 Umemura, K., Kawai, S. (2007). Modification of chitosan by the Maillard reaction using
890 cellulose model compounds. *Carbohydrate Polymers*, **68**, 242-248.
891 Umemura, K., Kawai, S. (2008). Preparation and characterization of Maillard reacted chitosan
892 films with hemicellulose model compounds. *Journal of Applied Polymer Science*, **108**,
893 2481–2487.
894 Vilela, C., Kurek, M., Hayouka, Z., Röcker, B., Yildirim, S., Antunes, M.D.C., Nilsen-Nygaard,
895 J., Pettersen, M.K., C.S.R. Freire. (2017). A concise guide to active agents for active food
896 packaging. *Trends in Food Science & Technology*, **80**, 212-222.
897 Vlacha, M., Giannakas, A., Katapodis, P., Stamatis, H., Ladavos, A., Barkoula, N.M. (2016).
898 On the efficiency of oleic acid as plasticizer of chitosan/clay nanocomposites and its role
899 on thermo-mechanical, barrier and antimicrobial properties – comparison with glycerol.
900 *Food Hydrocolloids*, **57**, 10–19.
901 Wang, Y., Liu, F., Liang, C., Yuan, F., Gao, Y. (2014). Effect of Maillard reaction products on
902 the physical and antimicrobial properties of edible films based on ε-polylysine and
903 chitosan. *Journal of the Science of Food and Agriculture*, **94**, 2986-2991.

Wu, S., Hu, J., Wei, L., Du, Y., Shi, X., Zhang, L. (2014). Antioxidant and antimicrobial activity of Maillard reaction products from xylan with chitosan/chitooligomer/glucosamine hydrochloride/taurine model systems. *Food Chemistry*, **148**, 196-203.

Xu, Z.Z., Huang, G.Q., Xu, T.C., Liu, L.N., Xiao, J.X. (2019). Comparative study on the Maillard reaction of chitosan oligosaccharide and glucose with soybean protein isolate. *International Journal of Biological Macromolecules*, **131**, 601-607.

Yildirim, A., Mavi, A., Kara, A.A. (2001). Determination of antioxidant and antimicrobial activities of *Rumex crispus* L. extracts. *Journal of Agricultural and Food Chemistry*, **49**, 4083–4089.

Zhai, L., Bai, Z., Zhu, Y., Wang, B., Luo, W. (2018). Fabrication of chitosan microspheres for efficient adsorption of methyl orange. *Chinese Journal of Chemical Engineering*, **26**, 657–666.

Zhang, H., Yang, J., Zhao, Y. (2015). High intensity ultrasound assisted heating to improve solubility, antioxidant and antibacterial properties of chitosan-fructose Maillard reaction products. *LWT - Food Science and Technology*, **60**, 253-262.

Zhang, N., Chen, H., Zhang, Y., Ma, L., Xu, X. (2013). Comparative studies on chemical parameters and antioxidant properties of stipes and caps of shiitake mushroom as affected by different drying methods. *Journal of the Science of Food and Agriculture*, **93**, 3107–3113.

Zhong, L., Ma, N., Wu, Y., Zhao, L., Ma, G., Pei, F., Hu, Q. (2019). Characterization and functional evaluation of oat protein isolate-*Pleurotus ostreatus* β-glucan conjugates formed via Maillard reaction. *Food Hydrocolloids*, **87**, 459-469.

Supplementary data

Click here to download Supplementary data: Supplementary Data CP R2.pdf

Graphical Abstract

Click here to download high resolution image

Sfax, 01th of March 2020

Credit author statement

Marwa HAMDI: Conceptualization, Methodology, Validation, Formal analysis, Investigation, Writing-Editing, Visualization.

Rim NASRI: Resources, Supervision.

Youssra BEN AZAZA: Investigation.

Suming LI: Resources, Supervision.

Moncef NASRI: Resources, Supervision, Review.

Dr. Marwa HAMDI

Laboratory of Enzymatic Engineering and Microbiology, National School of Engineers of Sfax, Sfax. B.P.1173, 3038 Sfax, Tunisia.

E-mail: marwahamdi50@yahoo.fr